

Abscopal Effect in Non-injected Tumors Achieved with Cytokine-Armed Oncolytic Adenovirus

Riikka Havunen,^{1,2} João M. Santos,^{1,2} Suvi Sorsa,^{1,2} Tommi Rantapero,³ Dave Lumen,⁴ Mikko Siurala,^{1,2} Anu J. Airaksinen,⁴ Victor Cervera-Carrascon,^{1,2} Siri Tähtinen,¹ Anna Kanerva,^{1,5} and Akseli Hemminki^{1,2,6}

¹Cancer Gene Therapy Group, Faculty of Medicine, University of Helsinki, Helsinki, Finland; ²TILT Biotherapeutics Ltd., Helsinki, Finland; ³BioMediTech, University of Tampere, Tampere, Finland; ⁴Laboratory of Radiochemistry, Department of Chemistry, University of Helsinki, Helsinki, Finland; ⁵Department of Obstetrics and Gynecology, Helsinki University Hospital, Helsinki, Finland; ⁶Comprehensive Cancer Center, Helsinki University Hospital, Helsinki, Finland

Cancer treatment with local administration of armed oncolytic viruses could potentially induce systemic antitumor effects, or the abscopal effect, as they self-amplify in tumors, induce danger signaling, and promote tumor-associated antigen presentation. In this study, oncolytic adenovirus coding for human tumor necrosis factor alpha (TNF- α) and interleukin-2 (IL-2) Ad5/3-E2F-d24-hTNF- α -IRES-hIL-2 (also known as [a.k.a.] TILT-123) provoked antitumor efficacy in tumors that were injected with Ad5/3-E2F-d24-hTNF- α -IRES-hIL-2 and those that were left non-injected in the same animal. Importantly, the virus was able to travel to distant tumors. To dissect the effects of oncolysis and cytokines, we studied replication-incompetent viruses in mice. Systemic antitumor effects were similar in both models, highlighting the importance of the arming device. The cytokines induced positive changes in immune cell infiltrates and induced the expression of several immune-reaction-related genes in tumors. In addition, Ad5/3-E2F-d24-hTNF- α -IRES-hIL-2 was able to increase homing of adoptively transferred tumor-infiltrating lymphocytes into both injected and non-injected tumors, possibly mediated through chemokine expression. In summary, local treatment with Ad5/3-E2F-d24-hTNF- α -IRES-hIL-2 resulted in systemic antitumor efficacy by inducing immune cell infiltration and trafficking into both treated and untreated tumors. Moreover, the oncolytic adenovirus platform had superior systemic effects over replication-deficient vector through spreading into distant tumors.

INTRODUCTION

Eight million cancer deaths occur globally each year, and almost all of them result from metastatic cancer.¹ New therapeutic approaches are thus urgently needed. Because the patients in need of novel treatments typically have metastatic disease, systemic therapeutic efficacy is required. After a century of developing immunotherapies, the first products have recently entered routine use. Many of them, including monoclonal checkpoint blocking antibodies and recombinant cytokines, are used systemically, which can cause severe adverse events and even mortality by affecting normal tissues.^{2,3} In contrast, the

typical embodiment of oncolytic immunotherapy is a local injection into tumors. Several types of oncolytic viruses are being investigated in preclinical and clinical studies, and one product, talimogene laherparepvec (also known as [a.k.a.] T-Vec or Imlygic), has already been approved.⁴⁻⁶ Even though T-Vec is not capable of spreading to distant tumors, local injection causes immunological reactions in distant metastases, a phenomenon known as abscopal effect.^{6,7}

The abscopal effect has been proposed as potentially relevant in patients being treated with systemic immunotherapy, such as checkpoint blocking antibodies, and local radiation.^{8,9} The biological rationale is that radiation can cause immunogenic cell death, allowing the induction of new T cells against the tumor, while concurrent checkpoint inhibitors prevent immunosuppression from occurring. This approach is now being tested in dozens of trials.¹⁰ Oncolytic viruses, such as T-Vec, are able to induce an abscopal effect without the need for radiation.^{6,7} The biological rationale is the same: oncolytic replication can induce immunogenic cell death and immunological danger signaling, both of which can induce *de novo* immunity against the tumor.

With regard to oncolytic viruses under development, but not yet approved (except oncolytic adenovirus Oncorine in China), oncolytic adenoviruses are well tolerated in humans and excellent devices for transgene delivery.^{5,11,12} For example, toxic systemic delivery of IL-2, regularly used in adoptive cell therapy protocols, is replaceable with virus-vectored IL-2 gene therapy in the context of T cell transfer.¹³ In addition to immune stimulation by the transgene, adenoviral oncolysis induces immunogenic cell death and the release of danger signals and tumor-associated antigens, which increase tumor immunogenicity.¹⁴⁻¹⁶ Importantly, adenovirally delivered cytokines provide enhanced antitumor efficacy with minimal or nonexistent toxicity.^{13,17}

Received 31 October 2018; accepted 31 October 2018;
<https://doi.org/10.1016/j.omto.2018.10.005>.

Correspondence: Akseli Hemminki, Cancer Gene Therapy Group, Faculty of Medicine, University of Helsinki, Haartmaninkatu 3, 00290 Helsinki, Finland.
E-mail: akseli.hemminki@helsinki.fi



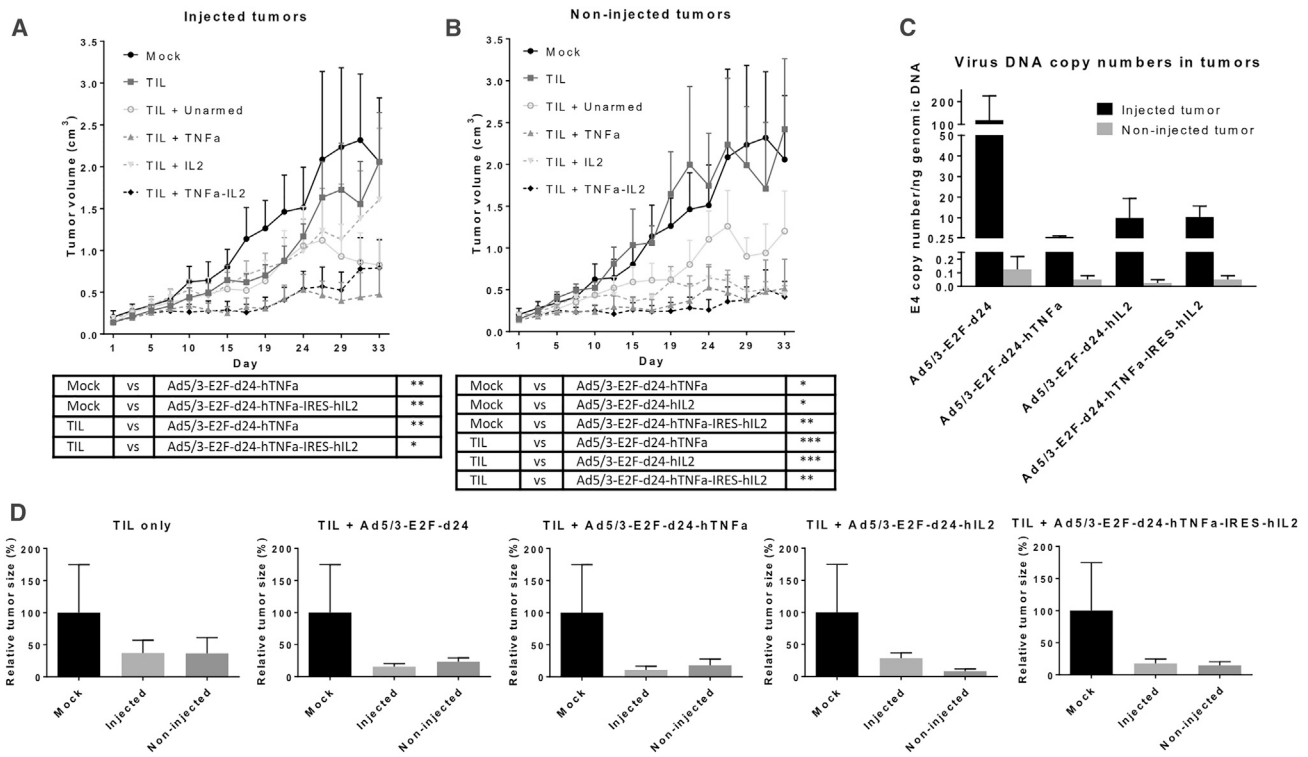


Figure 1. Treatment with Oncolytic Virus Controls the Growth of Both Injected and Non-injected Tumors

Hamsters were treated on days 1, 8, 15, 22, and 29 with 1×10^8 VPs intratumorally (i.t.) and with 5×10^7 TILs on day 1 intraperitoneally (i.p.). The growth of injected (A) and non-injected (B) hamster tumors ($n = 5-6$) was measured every 2-3 days until day 33. During the follow-up period, two animals were sacrificed from the mock group (day 24), two animals from the group receiving TILs only (day 22), and one animal from groups treated with Ad5/3-E2F-d24-hTNF- α (day 29) and Ad5/3-E2F-d24-hIL-2 (day 29). Small amounts of viral DNA were detectable also in non-injected tumors on day 16 (C). There were no differences between the injected and non-injected tumor sizes on day 33 (D). The graphs show mean plus SEM. Statistical differences were evaluated with mixed model analysis; **** $p < 0.0001$; *** $p < 0.001$; ** $p < 0.01$; * $p < 0.05$.

To decrease the toxicity and increase the efficacy of T cell-related immunotherapies, such as adoptive cell therapy and checkpoint inhibitors, we have developed an oncolytic adenovirus coding for human tumor necrosis factor alpha (TNF- α) and interleukin-2 (IL-2) (Ad5/3-E2F-d24-hTNF- α -internal ribosome entry site [IRES]-hIL-2, a.k.a. TILT-123).¹⁷⁻¹⁹ We hypothesized that oncolytic adenovirus replication accompanied by IL-2 and TNF- α production from tumor cells induces immunological effects that are powerful not only locally but also system-wide. Because we have seen Ad5/3-E2F-d24-hTNF- α -IRES-hIL-2 inducing positive changes locally in the tumor-infiltrating immune cell milieu, as well as on a systemic level,¹⁷ we studied whether a local treatment would be able to generate an abscopal effect on distant tumors and the mechanisms behind it.

RESULTS

Cytokine-Armed Oncolytic Adenoviruses Induce Systemic Antitumor Responses

The systemic effects of a local treatment with oncolytic Ad5/3-E2F-d24-hTNF- α -IRES-hIL-2 were studied in Syrian hamsters that are semi-permissive for human adenovirus replication.²⁰ In addition, certain human cytokines, including TNF- α and IL-2, are bioactive in hamsters.^{17,20} Because this virus was developed to enable T cell

therapies, the experimental settings included a treatment with tumor-infiltrating lymphocyte (TIL) graft. We observed tumor growth reduction in both injected and non-injected tumors without differences in tumor sizes between these tumors (Figures 1A, 1B, and 1D).

The arming devices resulted in a benefit in tumor control over the respective unarmed virus. With regard to injected tumors, the best groups were Ad5/3-E2F-d24-hTNF- α and Ad5/3-E2F-d24-hTNF- α -IRES-hIL-2 ($p = 0.002$ and $p = 0.0034$ compared with TILs alone, respectively; $p = 0.002$ and $p = 0.01$ compared with mock). Regarding non-injected tumors, all armed viruses had enhanced antitumor efficacy at the non-injected site, unlike the unarmed virus, when compared with mock and TILs alone (TIL versus TIL + TNF- α : $p = 0.001$; TIL versus TIL + IL-2: $p = 0.000427$; TIL versus TIL + TNF- α -IL-2: $p = 0.00007$; mock versus TIL + TNF- α : $p = 0.011$; mock versus TIL + IL-2: $p = 0.022$; mock versus TIL + TNF- α -IL-2: $p = 0.006$).

The viruses were present in injected tumors at high levels on day 16, 8 days after the last intratumoral injection. The highest values were observed in the group treated with the unarmed virus (Figure 1C). Viral DNA levels were low in non-injected tumors and normal tissues

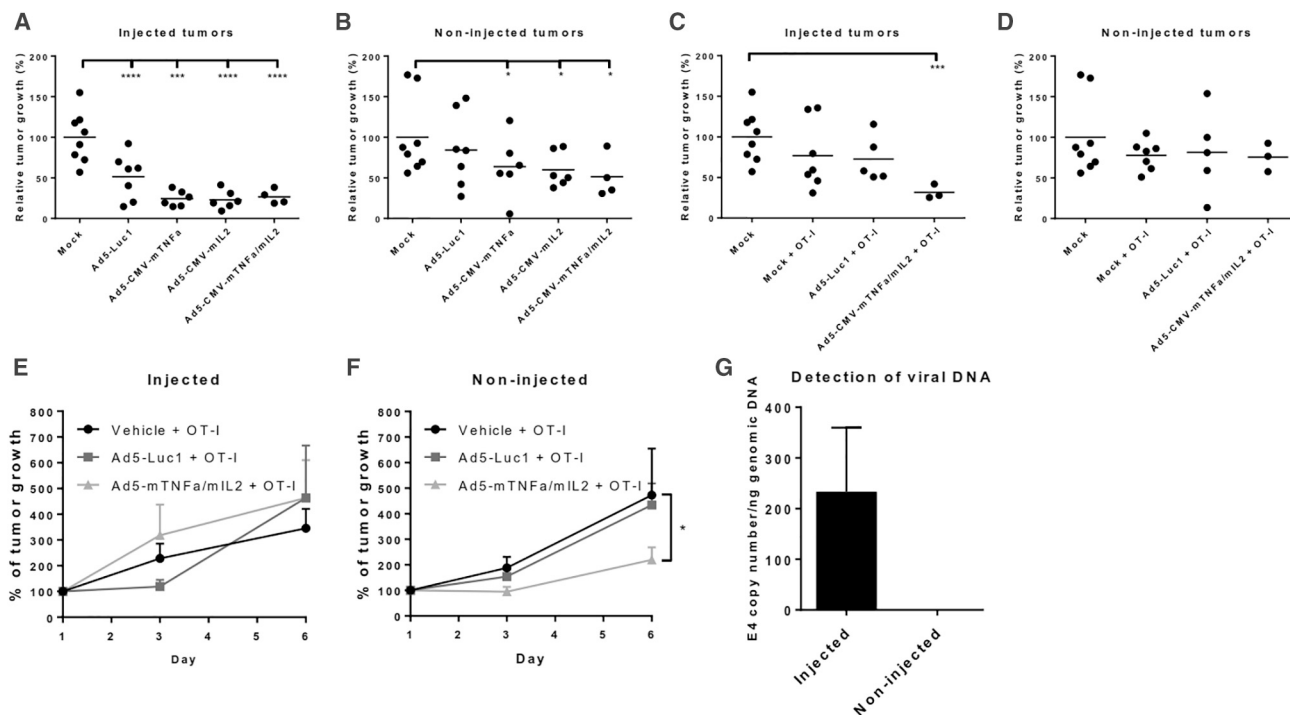


Figure 2. Replication-Incompetent Virus Induces Growth Control Also in the Non-injected Tumor at an Early Time Point

The sizes of injected (A and C) and non-injected (B and D) B16-OVA tumors in mice on day 8 ($n = 3-8$) without T cell transfer (A and B) or with OT-I cells (C and D) were compared with average mock tumor size on the same time point. Similar results were obtained for injected (E) and non-injected (F) tumors when the experiment was repeated. Viral DNA was detected only in the injected tumors (G). The bars show mean plus SEM. Statistical significance was evaluated with 2-way ANOVA: **** $p < 0.0001$; *** $p < 0.001$; * $p < 0.05$.

(Figures 1C and S1A). The highest individual values were detected in spleen, liver, and lung, but there were no differences in biodistribution between viruses or organs.

After treatments, animals were monitored and sacrificed according to animal regulations (tumor size reaching 20 mm). The group treated with the double-armed virus had the best survival ($p = 0.03$ and $p = 0.0159$ compared with mock and TILs alone, respectively), whereas TILs alone had a minimal effect on survival (Figure S1B).

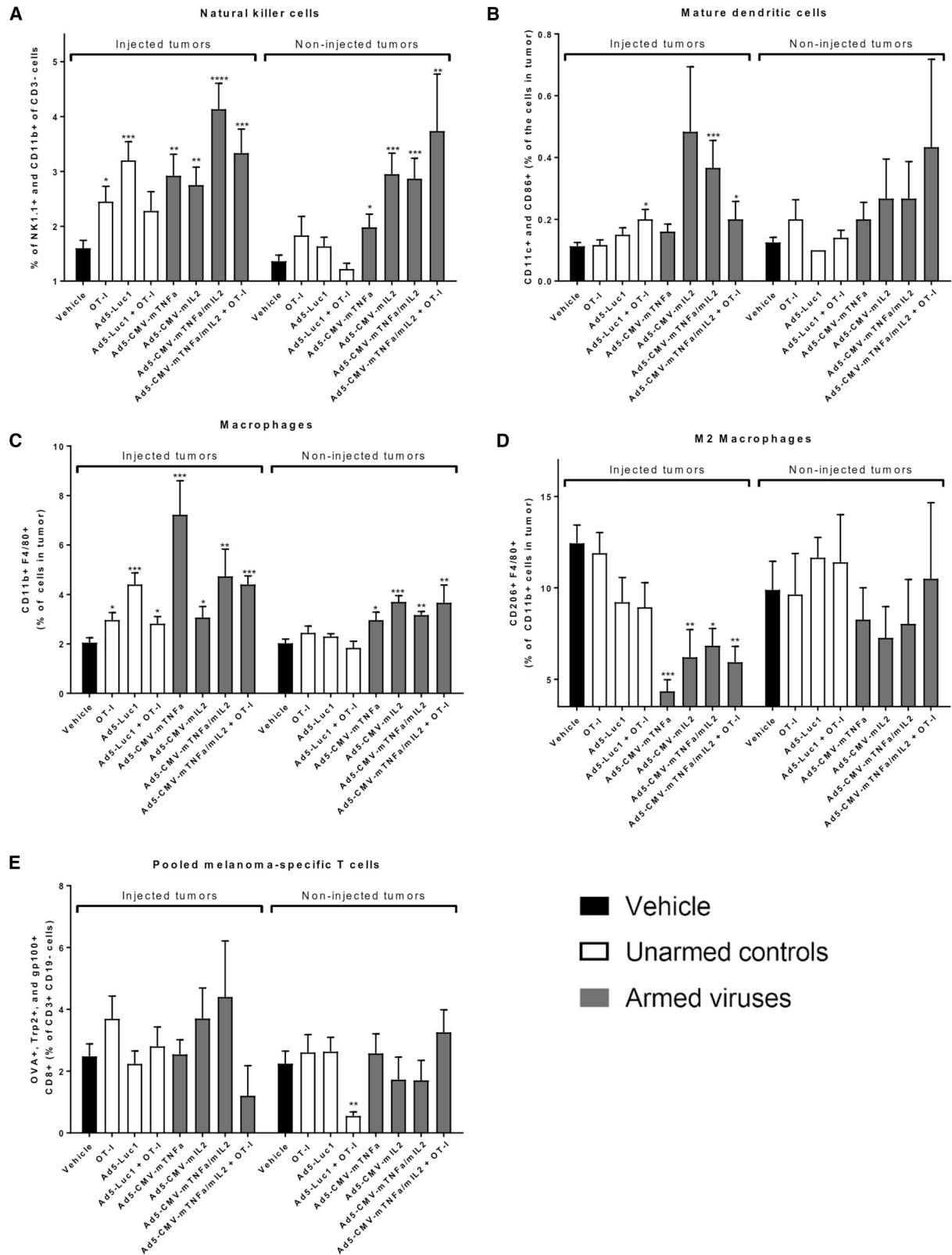
Arming with TNF- α and IL-2 Results in an Abscopal Effect Even without Oncolysis

Next, we sought to dissect the effect of the transgenes from the effects of oncolysis. This could be achieved by using replication-incompetent adenoviruses with murine cytokines in immunocompetent mice bearing B16 melanoma tumors expressing chicken ovalbumin (OVA). By day eight, an early time point, a difference in tumor size could be seen in both injected and non-injected tumors (Figures 2A and 2B). The tumors injected with IL-2- and TNF- α -armed viruses were about 70% smaller than the PBS-injected vehicle control tumors ($p < 0.0001$). The control virus Ad5-Luc1, which lacks an immunologically active transgene, had a minor yet statistically significant effect ($p = 0.0004$).

Regarding non-injected tumors, the armed viruses were the only ones able to induce tumor growth control (vehicle versus Ad5-CMV-mTNF- α : $p = 0.0162$; vehicle versus Ad5-CMV-mIL-2: $p = 0.0475$; vehicle versus Ad5-CMV-mTNF- α /mIL-2: $p = 0.0212$). The best tumor control was induced by the combination of the cytokines, mean tumor size being half of the size of the vehicle tumors. The addition of OVA-specific OT-I T cells resulted in similar outcomes but did not enhance tumor growth control at this early time point (Figures 2C and 2D).

The experiment was repeated with the most relevant treatments: OT-I T cells with vehicle control, control virus Ad5-Luc1, and Ad5-CMV-mTNF- α /mIL-2. Tumor growth was followed for 6 days. The treatment did not influence the growth of injected tumors, but the animals treated with cytokine-armed viruses clearly showed a delay in non-injected tumor growth as compared with vehicle treatment ($p = 0.04$; Figures 2E and 2F). Of note, the effect was not due to virus spread because viral genomes at the non-injected tumors were undetectable (Figure 2G). Thus, the viral transduction of distant tumors seems to require oncolysis and subsequent shedding of the virus from tumors into blood.

Day eight tumors were collected and analyzed for intratumoral immune cell populations. The percentage of natural killer (NK) cells



(legend on next page)

(NK1.1. and CD11b double-positive cells in the CD3-negative cell population) was elevated in both injected and non-injected tumors following treatment with cytokine-coding viruses (Figure 3A). In addition, the cytokine combination was able to increase the levels of CD11c- and CD86-positive dendritic cells in treated tumors, and the trend was similar in non-injected tumors (Figure 3B). Moreover, there was a positive correlation between the presence of NK cells and dendritic cells (Figures S2A and S2B).

An increase of F4/80 and CD11b-positive macrophages was observed in both tumors (Figure 3C). Interestingly, the portion of immunosuppressive M2-like macrophages (differentiated by CD206 expression) was decreased when tumors received cytokine-coding viruses (Figure 3D). Again, a similar, yet not significant, trend was seen in non-injected tumors. Out of other markers for immunosuppression, the treatments did not affect the expression of TGF- β or FoxP3 (Figures S2C and S2D). No major differences were observed between the groups regarding melanoma-specific (OVA, Trp2, and gp100) CD8-positive T cells (Figure 3E). The presence of any of the immune cell populations studied here did not correlate with tumor volumes (Figures S2E–S2J).

Armed Adenovirus Induces the T Cell Graft Trafficking into Both Injected and Non-injected Tumors

Because the oncolytic virus was able to travel to the non-injected tumors, we wanted to study whether the virus induces TIL graft trafficking into both injected and non-injected tumors. Distribution and tumor accumulation of the radiolabeled cells (^{111}In -oxine) were determined by single-photon emission computed tomography/computed tomography (SPECT/CT) imaging at 48, 72, and 96 hr after administration (Figures 4A and 4B). A trend of increased trafficking into both injected and non-injected tumors was observed in animals treated with Ad5/3-E2F-d24-hTNF- α -IRES-hIL-2 compared with the unarmed virus and the vehicle control (Figure 4C). In addition, the cells seemed to be more persistent in the tumors when the animals were treated with the cytokine-armed virus: there was no decrease over time in the injected or non-injected tumors, whereas in the vehicle and unarmed virus control groups the signal decreased over time.

To estimate the effect of the cytokines on T cell graft trafficking, fluorescently labeled OT-I T cells were administered to animals receiving vehicle, Ad5-Luc1 control virus, or Ad5-CMV-mTNF- α /IL-2 into one of the two tumors. Five days later, the tumors were collected and the presence of transferred T cells detected with flow cytometry. Even in the absence of oncolysis, treatment of one tumor was able to induce OT-I cell trafficking into both injected and non-injected

tumors (Figure 4D). The transferred T cells did not find their way into the tumors when the animals were treated with vehicle control, and only a low signal was detected in non-injected tumors in animals receiving the control virus. There were no statistically significant differences between the injected and non-injected tumors.

Oncolytic Adenovirus Induces the Expression of Immunologically Relevant Genes in Injected and Non-injected Tumors

In order to uncover the mechanisms of action underlying the systemic effects and the trafficking of adoptively transferred cell graft, we analyzed the gene expression profiles of injected and non-injected tumors in hamsters receiving TIL therapy. In the vehicle group, PBS injection induced immune reactions by the upregulation of the genes related to humoral immune responses, chemokine and cytokine production, inflammatory responses, and complement activation, among others (Table S1). In addition, the PBS injection downregulated genes related to cytoskeleton organization and other filament-related processes. To allow for the effects of the needle puncture and vehicle injection, we analyzed treatment group expression levels against corresponding vehicle group tumors.

Over 2-fold upregulation was observed for 445 genes in injected tumors and for 165 genes in non-injected tumors (Figures S3 and 5). The number of downregulated genes was 45 and 70 in injected and non-injected tumors, respectively (Figures S3 and 6). TIL treatment without viruses induced the expression of chemokines (*Ccl4*, *Ccl7*, *Ccl11*), but also immune checkpoint molecules *Pdl1* (or *Cd274*) in the PBS-injected tumors and *Lag3* in the non-injected tumors. In addition, we saw upregulation of a variety of lymphocyte-related genes (*Sash3*, *Fgl2*, *Txk*, *Gzmk*, *Bst1*, *Pik3ap1*, *Pik3cd*, *Prkcb*, *Nkg7*, *Spn*), T cell activators (*Prkca*, *Tagap*) and inhibitors (*Ptprc*, *Ptpn22*), dendritic cell marker *Irga3* (or *Cd11c*), genes promoting cytokine production (*Themis2*, *Fgr*, *Trem1*), and *Rnf144b*, whose product functions in major histocompatibility complex (MHC) class I antigen processing and presentation (Figures 5 and S5).

Virus Injection Induces the Upregulation of Genes Related to Both Innate and Adaptive Immunity

Out of immunologically relevant genes, injection with either virus induced the expression of macrophage marker *Scara5*, chemokine gene *Cxcl12*, lymphocyte differentiation marker *Nt5e*, and two genes, *Retnla* and *Retnlb*, related to T cell and dendritic cell recruitment, respectively. In addition, we saw upregulation of T cell inhibitor *Ido1* in non-injected tumors in the group treated with the unarmed virus and TILs. In addition, as seen in mice, virus injection was

Figure 3. Treatment with Armed Viruses Induces Positive Changes in Immune Cells in the Tumor Microenvironment

Tumor samples were collected on day 8, and the presence of natural killer cells (A), mature dendritic cells (B), macrophages (C), and M2-like macrophages (D) in tumors was detected with flow cytometry. Melanoma-specific T cells were detected with pentamers and the results with OVA⁺, Trp2⁺, and gp100⁺ cells pooled into one graph (E). Statistical differences were analyzed against corresponding mock tumor. The bars show mean plus SEM. Black bar indicates mock control, white bars unarmed virus or OT-I controls, and gray bars treatment groups with armed viruses. Unpaired t test was performed to analyze statistical differences; ****p < 0.0001; ***p < 0.001; **p < 0.01; *p < 0.05.

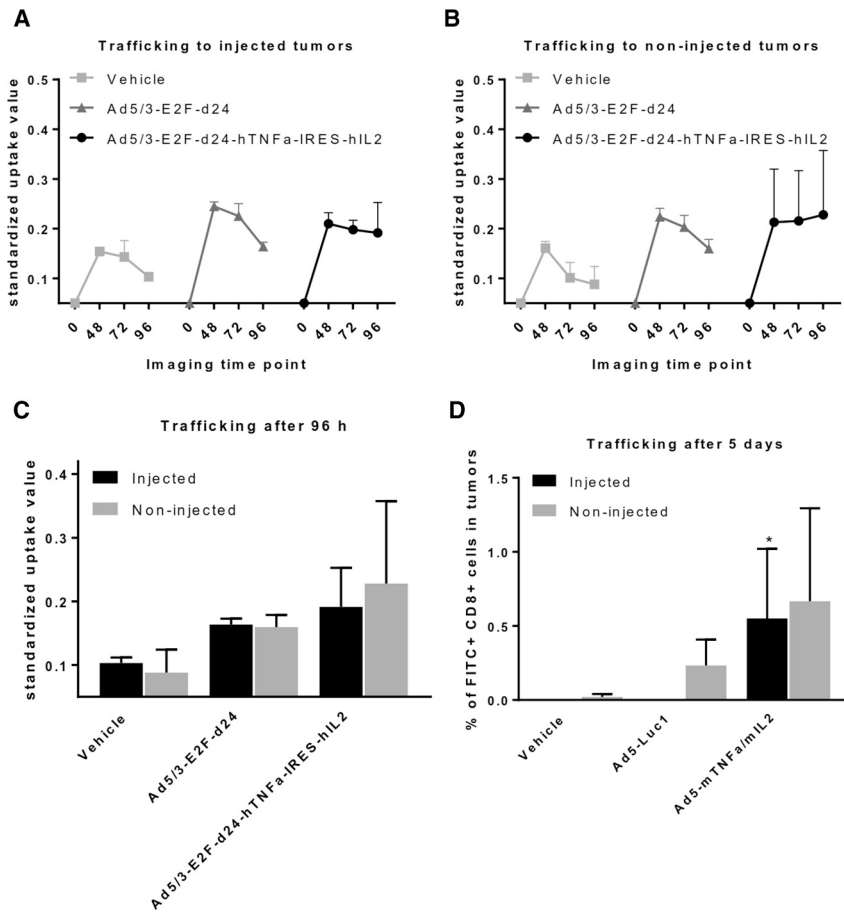


Figure 4. Armed Virus Induces TIL and TCR Graft Trafficking to and Persistence in Both Tumors

TILs were labeled with radioactive indium, and the trafficking into (A) injected and (B) non-injected tumors was followed with SPECT/CT imaging over time. On day 0, the hamsters received the labeled TILs intraperitoneally and viruses or PBS control intratumorally into one of the two tumors ($n = 2/\text{group}$). The difference between the groups was most prominent 96 hr after the administration of the cells (C). TCR-modified OT-1 cells were labeled with fluorescent-labeled nanoparticles, and their presence in injected and non-injected tumors was investigated after 5 days ($n = 6$) (D). Tumors injected with viruses coding for TNF- α and IL-2 had significantly higher numbers of infused OT-1 cells compared with vehicle-treated tumors (Kruskal-Wallis test, $*p < 0.05$).

tion of macrophage-related gene *Marco*, and *Ackr3* coding for an atypical chemokine receptor. In the same group, the non-injected tumors showed upregulation of immunoglobulin lambda- and kappa-like genes. When expanding the observations to all significantly differentially expressed genes present both in injected and non-injected tumors uniquely in this group, we observed upregulation of *Cxcl5* coding for TNF- α -inducible chemokine and *Rnase2* that attracts dendritic cells (Table S2). Furthermore, we saw upregulation of the following genes related to immune reactions: *Ier3* that has

functions in TNF- α -stimulated apoptosis and T cell apoptosis inhibition; *Lrmp*, whose protein product delivers peptides to MHC class I molecules; B cell regulator *Rgs13*; and *Sult1e1* that is involved in inflammatory-response regulation. By contrast, immune-reaction-related genes that were downregulated in this group in both tumors were *Jak3* (mediates IL-2R signaling in T cells and NK cells) and three genes coding for parts of MHC class II complex (Table S2).

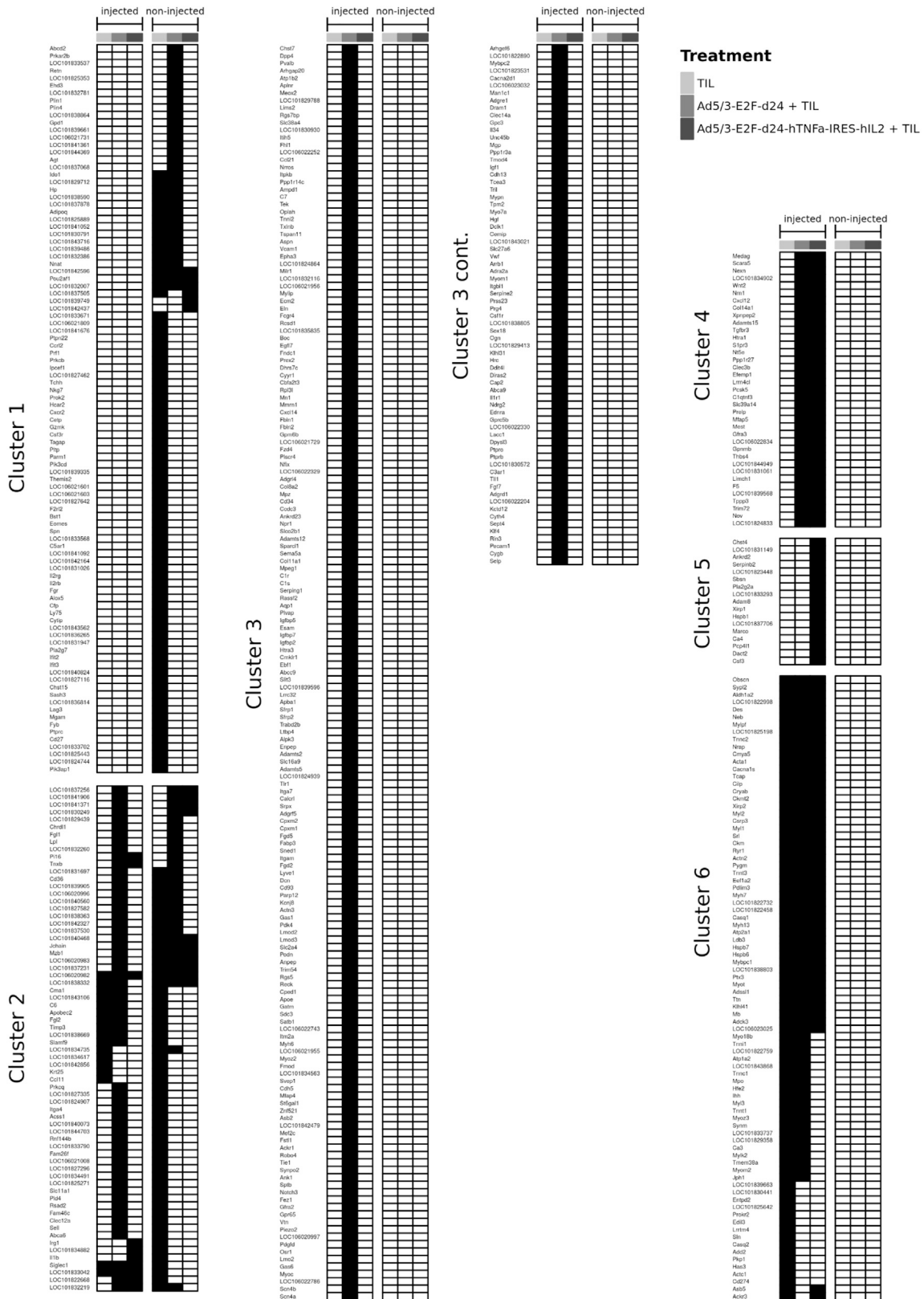
Because the double-armed virus had more prominent antitumor abscopal effects on the non-injected tumors in comparison to the same virus without arming devices, it was of interest to study those genes that changed only in non-injected tumors, and only when the double-armed virus was used for injection of the other tumor. In theory, this could allow dissection of the abscopal effects of oncolysis from the effects of the transgenes. However, only a few such genes were identified (upregulation of LOC101839749 and LOC101842437, annotated as immunoglobulin lambda-1 light chain-like and immunoglobulin kappa variable 4-1-like, respectively, and downregulation of *Ca3*, *Mylpf*, *Ckm*, and *Hspb1*), but they are currently of unknown significance in the context of immunotherapy. Further cell biology research could eventually help understand the role of these transcripts in our findings.

able to upregulate NK cell activation markers and dendritic cell differentiation (Figure S5).

The unarmed virus induced the upregulation of the highest number of genes. Among the genes upregulated in the unarmed group, there were several T cell markers (*Itm2a*, *Prckq*, *Dpp4*, *Aplnr*), B cell-related genes (*Jchain*, *Ebf1*, *Fgd2*, *Mzb1*), chemokines and their receptors (*Ccl21*, *Ackr1*, *Ccr5*, *Cmklr1*, *Cxcl14*), complement system-related genes (*C1s*, *C1r*, *C3ar1*, *C4*, *C6*, *C7*), and antigen presentation-related genes (*B2m*, *Tap1*, *Tap2*, *Tapbp*; Figure S4). Interestingly, Ad5/3-E2F-d24 also upregulated genes that are required for lymphocyte migration and invasion, such as *Vcam1*, *Pecam1*, and *Esam*, in addition to *CD34* and *Sell*, coding for the binding partner of CD34 on T cells, L-selectin. Another interesting detail unique to the unarmed virus was the upregulation of genes related to viral processes, for example, antiviral *Rsad2* (Figure S5). In addition, we saw downregulation of inflammation-related genes such as *S100a9*, *S100a8*, *Orm1*, *Ltb* (or *Trfc*), and *Gc* (Figures 6 and S6).

Armed Adenovirus Induces Chemokine Expression in Both Injected and Non-injected Tumors

Tumors injected with armed virus showed unique upregulation of cytokine genes *Csf3* and *Il1b*. In addition, we saw an upregula-



(legend on next page)

DISCUSSION

Cytokines, such as TNF- α and IL-2, are potent inducers of antitumor immunity. TNF- α has both direct and indirect effects on cancer cells by inducing necrosis and apoptosis, but also inducing immunologic reactions via acute inflammation.²¹ Recombinant TNF- α is routinely used in isolated limb perfusion of, for example, sarcoma and melanoma, but it is too toxic to be used systemically.^{22,23} With adenoviral delivery, high local concentration of TNF- α and IL-2 is achievable without significant systemic exposure.^{17,18} IL-2 functions as a T cell propagator and activator, and it is used as a treatment for melanoma and renal cell carcinoma. IL-2 is also included in many adoptive cell therapy trials, especially in TIL therapy and in many solid tumor trials with chimeric antigen receptor T cells (CART) or with receptor-modified T cells (TCR).^{24–26} Again, vectored delivery can achieve the beneficial effects of IL-2 without systemic toxicity.¹³ Here, we inserted TNF- α and IL-2 into an oncolytic adenovirus and studied the systemic antitumor effects of Ad5/3-E2F-d24-hTNF- α -IRES-hIL-2 with adoptive T cell transfer.

Oncolytic adenoviruses whose capsid is a chimera between serotype 5 and serotype 3 appear useful with regard to systemic delivery. In line with the results obtained in this study, we have previously shown in both laboratory animals and humans that virus administered intratumorally or intravenously can transduce distant metastases.^{11,27} It has even been possible to grow out the treatment virus from non-injected brain metastases of a cancer patient.¹¹ Injected and non-injected tumors were transduced to the same degree in patients. Thus, the 5/3 chimeric platform is appealing for achieving systemic effects also through viral transduction, in addition to immunological effects.

Consistent with previous results, the oncolytic virus studied here could be detected in both injected and non-injected tumors. The virus spread was linked to replication, because the replication-incompetent viruses were not found in non-injected tumors. Oncolytic virus levels were higher in injected tumors than in non-injected tumors, but the presence in non-injected tumors in immune-competent hosts constitutes an important proof-of-concept. Moreover, the level of unarmed virus in injected tumors was higher than that of armed viruses, suggesting more extensive immunogenicity of the armed viruses. Because the viruses were found in non-injected tumors, it was not surprising to find them also in normal tissues. The selectivity of the virus, however, is not at the level of entry, but on the level of replication.²⁸ Because the virus does not replicate in normal cells, these cells are not damaged and no adverse events are seen.¹⁷ In fact, higher DNA copy number can sometimes be seen in normal human tissues than in tumors.¹¹

In contrast with oncolytic adenovirus, the first oncolytic virus approved by authorities in the United States and European Union (EU), T-Vec, has not been detected from non-injected tumors in

humans or in animals.²⁹ Nevertheless, T-Vec induces immunological responses in distant tumors, even though at a lower level.^{6,7} In the phase 3 OPTIM trial, T-Vec resulted in a 26% response rate in injected tumors and 15% in non-injected visceral metastases.⁶ Because our approach induced similar efficacy in injected and in non-injected tumors, one can speculate that overall clinical benefits could be more pronounced if the virus is capable of transducing non-injected tumors. Thus, there is a major difference between oncolytic herpes type 1 and oncolytic 5/3 chimeric adenovirus, and this difference is potentially very important clinically. The former can produce systemic effects through the immune system, whereas the latter can achieve body-wide effects through two mechanisms: (1) viral dissemination through the vasculature, transduction of distant tumors followed by transgene expression, and oncolysis; and (2) systemic immunological effects. Considering there are several oncolytic viruses in development, it is clear that they are not all alike with regard to the mechanisms of action and systemic efficacy.

As a result of virus spread into non-injected tumors, there were no significant differences between the sizes of injected and non-injected tumors in this study. Moreover, cytokine-armed viruses influenced circulating T cell graft seen as increased trafficking into distant tumors, both with oncolytic and replication-incompetent viruses. The experiment with replication-incompetent viruses without T cell therapy highlighted the importance of the transgenes in inducing the systemic antitumor effects. Even in the absence of oncolysis, the replication-incompetent viruses were able to inhibit the growth of the non-injected tumors when armed with TNF- α and IL-2. Moreover, with oncolytic viruses, the unarmed virus was not able to induce as strong antitumor effects as the armed viruses in the non-injected tumors despite higher copy number. The results are in line with our previous results with the same constructs: TNF- α and IL-2 are necessary for enabling curative treatment with TIL therapy and inducing immunological memory against tumor rechallenge.¹⁷ Here, the two different animal models, hamsters and mice, both suggest that the transgenes have an importance in inducing systemic antitumor effects.

Due to limited availability of hamster-specific or cross-reactive reagents, a mouse model provided us a means to study immune cell compartments in tumors, having the focus on innate immunity. Interestingly, treating just one tumor induced immune cell infiltration also into the non-injected tumor. Moreover, the presence of immune cells in tumors did not correlate with tumor sizes, suggesting that the treatment influences tumor microenvironment regardless of the volume. The clearest difference was seen with NK cells that are known to attack cells with low MHC class I expression, such as B16-OVA.^{30,31} The presence of any virus induced NK levels in the injected tumors, but an arming device was required for NK cell induction in the

Figure 5. List of Genes Upregulated over 2-Fold Compared with Corresponding Mock Group

Genes in cluster 1 are upregulated only in non-injected tumors, genes in cluster 2 are upregulated in both tumors, genes in cluster 3 are upregulated with Ad5/3-E2F-d24 injection, genes in cluster 4 are upregulated with either virus, genes in cluster 5 are upregulated with Ad5/3-E2F-d24-hTNF- α -IRES-hIL-2 only, and genes in cluster 6 with any injection. Black box indicates over 2-fold upregulation.

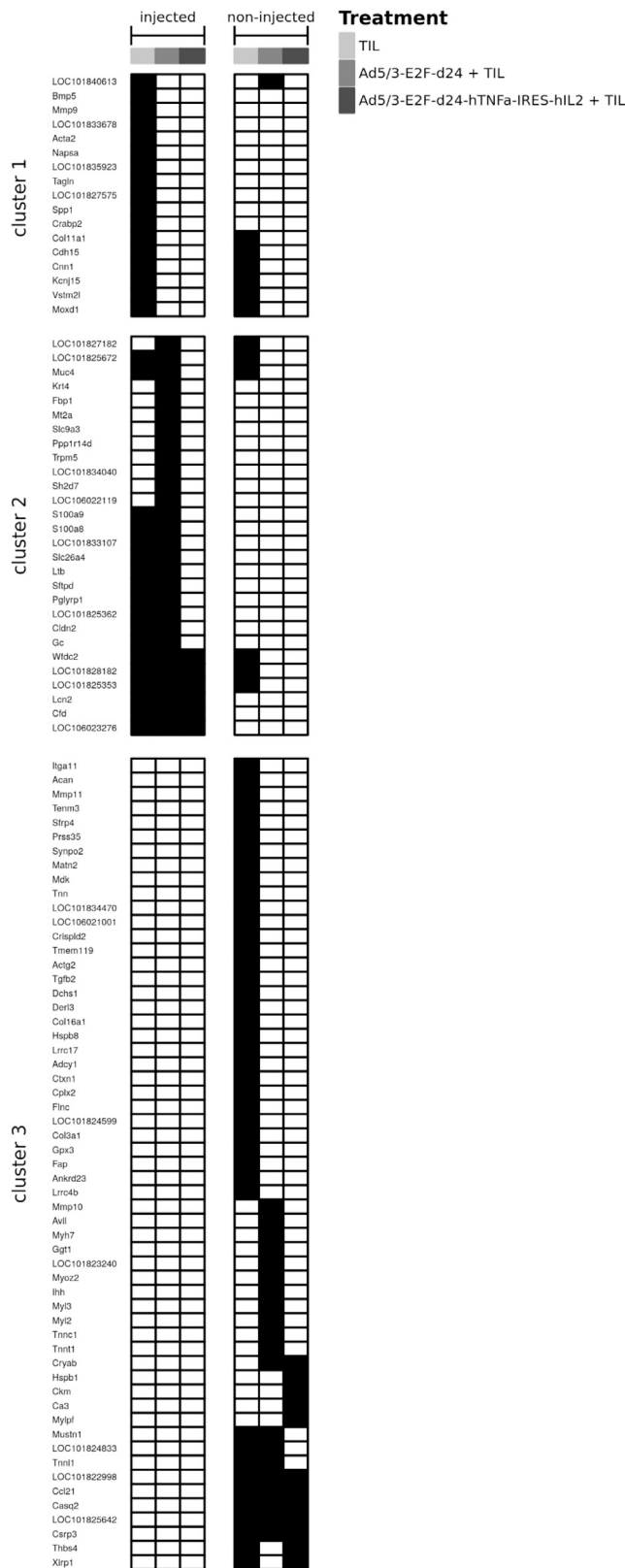


Figure 6. List of Genes Downregulated over 2-Fold Compared with Corresponding Mock Group

Genes in cluster 1 are downregulated in TIL group, genes in cluster 2 are downregulated with a virus injection, and genes in cluster 3 are downregulated only in non-injected tumors. Black box indicates over 2-fold downregulation.

non-injected tumor. Interestingly, also Balasa et al.³² reported the importance of the combination of IL-2 and TNF- α with regard to NK activation.

In addition to NK cells, IL-2 stimulated the presence of dendritic cells expressing the maturation marker CD86. Moreover, the presence of mature dendritic cells positively correlated with higher numbers of NK cells in the tumor. Crosstalk between NK cells and dendritic cells has an interesting role in both innate and adaptive immunity. NK cells promote tumor antigen presentation by dendritic cells, but at the same time, CD11c-positive dendritic cells are required for NK cell priming.^{33,34} Moreover, NK cells induce dendritic cell maturation both via cell-cell contacts and via secretion of TNF- α and interferon gamma.³⁵ NK cells additionally secrete chemokines, such as MIP-1 α , MIP-1 β , and RANTES, which attract dendritic cells.³⁶

In addition to inducing dendritic cell maturation, TNF- α is capable of suppressing the M2 macrophage phenotype.³⁷ Immunosuppressive M2-like macrophages are known to associate with poor survival in cancer patients, and cancer cells appear to attempt to drive macrophage differentiation toward this phenotype.^{38,39} We saw, however, a relative decrease in this subtype of macrophages when tumors were injected with armed viruses even though the overall macrophage percentage was increased in both tumors. The effect was most noticeable with TNF- α -coding virus. A similar trend was seen in gene expression profiles in hamster tumors where 12 out of 19 genes specific for M1 macrophages according to Kratochvill et al.³⁷ were upregulated in tumors treated with Ad5/3-E2F-d24-hTNF- α -IRES-hIL-2. Likewise, the expression of 13 out of 20 genes that are linked to M2 phenotype was absent in the tumors.

When interpreting gene expression data, it is important to extract the effects derived from the delivery of the drug. We have previously observed that injection with saline causes immunological reactions in tumors.⁴⁰ This phenomenon was confirmed in our observations with the upregulation of immune-reaction-related genes caused by injection of PBS. To control the effect of PBS injection, we compared the gene expression profiles of the virus-injected tumors with the saline-injected tumors and the non-injected tumors with the non-injected tumors in the vehicle group. Most changes in gene expression profile occurred in the group treated with the unarmed virus. Because this virus causes fewer immune responses toward tumor cells that allow replication, oncolysis is more prominent, and therefore the majority of the expression changes seen are due to this phenomenon. For example, the virus upregulated many of the complement system components, suggesting that the unarmed virus might have induced more antiviral immune responses than the armed virus.

The cytokines seemed to influence the trafficking and the persistence of the transferred cells in both injected and non-injected tumors, regardless of oncolysis. Previously, increased chemokine expression in the tumors treated with replication-incompetent adenoviruses armed with TNF- α and IL-2 was linked to increased T cell trafficking in mice.¹⁸ Here, we studied the effect of oncolytic viruses on chemotactic genes and genes promoting leukocyte proliferation and survival in both injected and non-injected tumors. Interestingly, many of these, such as *Cxcl5*, *Rnase2*, and *Ier3*, were uniquely upregulated in the group treated with Ad5/3-E2F-d24-hTNF- α -IRES-hIL-2.

In addition to chemokines, we saw upregulation of a set of genes related to different immune cell compartments, invasion of T cells through the vessels, and antigen presentation. Recently, Patel et al.⁴¹ reported extensive analysis of genes important for responses to immunotherapy in cancer. Interestingly, the same genes related to MHC class I antigen processing and presentation (*B2m*, *Tap1*, *Tap2*, and *Tapbp*) were upregulated in tumors injected with Ad5/3-E2F-d24 and in animals treated with TILs only. Moreover, they discovered that loss-of-function mutations in *Aplnr*, coding for apelin receptor, reduce the effectiveness of T cell therapies, including anti-CTLA4 blockade. Of note, in our dataset, *Aplnr* was upregulated in all the injected tumors and in the non-injected tumors in the group that received Ad5/3-E2F-d24. Of course, the efficacy of an immunotherapeutic does not depend on the expression of a single gene, but is a matter of inducing the right set of genes. Nevertheless, the correlation of our data with Patel's data is tantalizing, and because they used different methodology and made the observations from human data, the identified genes seem indeed relevant for cellular immunotherapy.

To conclude, our study demonstrates systemic effects induced by local injection of Ad5/3-E2F-d24-hTNF- α -IRES-hIL-2. The virus was able to spread to non-injected tumors, while the experiments with replication-incompetent viruses pointed out the importance of the arming device. Together, the oncolytic replication and the arming devices induced upregulation of genes essential for successful immunotherapy. Thus, an abscopal effect was seen and it was caused by two synergistic phenomena: (1) viral dissemination through the bloodstream into distant tumors, followed by oncolysis, and (2) systemic immune response. Taken together with previous reports, the findings presented here underline the rationale for using Ad5/3-E2F-d24-hTNF- α -IRES-hIL-2 as an enabler of T cell therapies and checkpoint inhibitors. A clinical trial, where the virus is used in patients receiving adoptive TIL therapy, is in progress.

MATERIALS AND METHODS

Cell Lines and Viruses

All cell lines were maintained under recommended conditions and tested to be pathogen-free. In mouse experiments, we used mouse melanoma cell line B16-OVA, a kind gift from Prof. Richard Wiley (Mayo Clinic, Rochester, MN, USA), and replication-deficient adenoviruses Ad5-CMV-mIL-2, Ad5-CMV-mTNF- α , and Ad5-Luc1.^{18,42} Oncolytic adenoviruses Ad5/3-E2F-d24, Ad5/3-E2F-d24-hTNF- α , Ad5/3-E2F-d24-hIL-2, and Ad5/3-E2F-d24-hTNF- α -IRES-IL-2¹⁷

were studied with hamster pancreatic cancer cell line HapT1 (DSMZ, Braunschweig, Germany).

Hamster Experiments

Oncolytic adenoviruses armed with human TNF- α and IL-2 were studied in Syrian hamsters (Envigo). 4×10^6 HapT1 cells were implanted on both flanks of the animals and allowed to develop for 7 days. Tumors were treated with 1×10^8 viral particles (VPs) intratumorally once a week and once with 5×10^7 HapT1-derived TILs administered intraperitoneally. As a control, one of the two tumors in the TIL group was treated with PBS, whereas the mock tumors were left untreated. The extraction of TILs is described previously.^{17,43} Four animals per group were sacrificed after two virus treatments on day 16, and tumors, heart, lung, liver, spleen, and kidney were collected from each animal to detect biodistribution of the virus with qPCR. Tumor sizes on the rest of the animals (5–6 per group) were followed for 122 days.

Mouse Experiments

The Experimental Animal Committee of the University of Helsinki and the Provincial Government of Southern Finland approved the animal experiments performed in this study. To investigate the effects of the adenovirally delivered transgenes, two B16-OVA tumors (2.5×10^5 cells each) were implanted into the flanks of C57BL/6 mice (Envigo, Cambridgeshire, UK). When the tumor size reached approximately 5 mm 10 days after the implantation, the animals were randomized into groups of 8–11 and treated intratumorally on days 1 and 4 with 1×10^9 VPs for single viruses or 0.5×10^9 VPs each when the virus coding for mIL-2 and mTNF- α were combined. The vehicle control group received PBS. CD8-enriched OVA-specific OT-I cells were processed as described previously⁴⁰ and administered 1.4×10^6 cells per animal intraperitoneally on day 1. The animals were sacrificed a week after the treatments, and tumors were collected for detecting the spread of the virus and the immune cell contents.

To investigate OT-I cell trafficking in mice, we labeled the cells with Qtracker 565 Cell Labeling Kit (Thermo Fisher Scientific, Waltham, MA, USA). The animals received intraperitoneally 7.6×10^5 cells, out of which 14% showed a positive fluorescent signal. One of the two B16-OVA tumors was injected with 50 μ L of PBS, 1×10^9 VPs of Ad5-Luc1 or Ad5-CMV-mTNF- α and Ad5-CMV-mIL-2 in a one-to-one ratio on days 1 and 3. Tumors were collected on day 6 and analyzed for fluorescein isothiocyanate (FITC)⁺ CD8⁺ cells, representing the transferred OT-I cells.

SPECT/CT Imaging

TILs were labeled with ¹¹¹In-oxine and administered intraperitoneally into Syrian hamsters (5×10^7 cells, 5.82 ± 0.73 MBq) bearing two HapT1 tumors ($n = 4$ /group). One of the two tumors received 1×10^8 VPs of Ad5/3-E2F-d24, Ad5/3-E2F-d24-TNF- α -IRES-IL-2, or 50 μ L of PBS as a control on day 0, and the animals were imaged with NanoScan SPECT/CT (Mediso, Budapest, Hungary) at 48, 72, and 96 hr after the administration of the cells. The results are reported as standardized uptake values (SUVs), which were calculated using

the average radioactivity concentration in the whole tumor normalized with the injected radioactivity dose and the animal weight. The tumors were delineated by using the co-registered CT images.

Gene Expression Profiling

To dissect the mechanisms of action on the gene expression level, we performed mRNA sequencing. Two of four subcutaneously established HapT1 tumors received virus and TIL treatments as described above. On day 10, 2 days after the last treatment, tumors were collected and stored in RNAlater (AM7020; Life Technologies, Thermo Fisher Scientific) before extracting RNA with RNeasy Mini Kit (74104; QIAGEN, Valencia, CA, USA). The library for sequencing was prepared with NEBNext Ultra Directional RNA Library Prep Kit 3 (E7420S; New England Biolabs, Ipswich, MA, USA) before performing single-end Illumina NextSeq High Output 1 × 75 bp sequencing (FC-404-2005; Illumina, San Diego, CA, USA).

The quality of the acquired data was analyzed with FastQ and summarized with MultiQC.^{45,46} Light quality trimming was performed with Trimmomatic.⁴⁷ The sample reads were aligned and annotated against RefSeq GCF_000349665.1_MesAur1.0_genomic reference and quantified with featureCounts.⁴⁸ Expression profiles of injected and non-injected tumors in the treatment groups were compared with corresponding tumors in the vehicle group, and the statistics for differentially expressed genes were calculated with DESeq2.⁴⁹ For each set of differentially expressed genes, obtained by comparing the treated group against the corresponding mock group (fold change > 1, $p < 0.05$), gene ontology analysis was performed against human orthologs with the WebGestalt toolkit.⁵⁰ The human orthologs were retrieved from the NCBI database.^{51,52}

In addition, the expression of TGF- β and FoxP3 were assessed from the RNA samples by qRT-PCR. The RNA was transcribed to cDNA with High-Capacity cDNA Reverse Transcription Kit (Thermo Fisher Scientific) according to manufacturer's instructions. The primer and probe sequences were adopted from Zivcec et al.,⁵³ and the results were normalized against GAPDH housekeeping gene as previously described.⁴⁴

Flow Cytometry

Dendritic cells, macrophages, NK cells, and melanoma marker (Trp2, gp100, and OVA)-specific T cells were detected from mouse tumor samples with flow cytometry as described by Tähtinen et al.⁵⁴

Virus Spread into Organs and Untreated Tumors

DNA was extracted from 25-mg tissue samples with QIAmp DNA Mini Kit (51326; QIAGEN), and the QIAcube machine according to the manufacturer's protocol. Adenoviral E4 was detected by qPCR as described earlier and normalized against hamster *GAPDH* or mouse β -actin gene expression.^{42,44}

Statistics

Tumor growth curves were analyzed with mixed model analysis in IBM SPSS Statistics version 22.0.0.1 (IBM, Armonk, NY, USA). Other

calculations were made with GraphPad Prism 7.03 (La Jolla, CA, USA). The survival benefit was evaluated with log rank test, and the other results were analyzed with ANOVA, Kruskal-Wallis test, or unpaired t test. All tests were performed as two-sided.

SUPPLEMENTAL INFORMATION

Supplemental Information includes six figures and two tables and can be found with this article online at <https://doi.org/10.1016/j.omto.2018.10.005>.

AUTHOR CONTRIBUTIONS

Conceptualization, R.H., M.S., S.S., S.T., and A.H.; Methodology, R.H., T.R., D.L., and A.J.A.; Investigation, R.H., J.M.S., S.S., D.L., and V.C.-C.; Formal Analysis, R.H. and T.R.; Writing – Original Draft, R.H.; Writing – Review & Editing, R.H., J.M.S., S.S., T.R., D.L., M.S., A.J.A., V.C.-C., S.T., A.K., and A.H.; Funding Acquisition, A.K. and A.H.; Resources, A.J.A. and A.H.; Supervision, A.H.

CONFLICTS OF INTEREST

A.H. is a shareholder in Targovax ASA. A.H. is an employee and shareholder in TILT Biotherapeutics Ltd. R.H., S.S., M.S., J.M.S., and V.C.-C. are employees of TILT Biotherapeutics Ltd.

ACKNOWLEDGMENTS

The authors thank Minna Oksanen and Susanna Grönberg-Vähä-Koskela for expert assistance. FACS Core Facility (Biomedicum Helsinki, Finland) provided the facilities and the technical assistance for flow cytometry, and Functional Genomics Unit FuGU (Biomedicum Helsinki, Finland) performed the mRNA sequencing and the related data analysis. SPECT/CT Imaging Core at Centre for Drug Research (Helsinki, Finland) is acknowledged for providing the facilities and expertise for imaging. The study was supported by University of Helsinki Doctoral Programme in Clinical Research, Cancer Foundation Finland, Jane and Aatos Erkko Foundation, HUCH Research Funds (EVO), Sigrid Jusélius Foundation, Finnish Cancer Organizations, University of Helsinki, TILT Biotherapeutics Ltd., and European Commission Marie Curie Innovative Training Network (ITN) grant VIRION (H2020-MSCA-ITN-2014 project number 643130).

REFERENCES

1. Seyfried, T.N., and Huysentruyt, L.C. (2013). On the origin of cancer metastasis. *Crit. Rev. Oncol.* 18, 43–73.
2. Gedye, C., van der Westhuizen, A., and John, T. (2015). Checkpoint immunotherapy for cancer: superior survival, unaccustomed toxicities. *Intern. Med. J.* 45, 696–701.
3. Schwartz, R.N., Stover, L., and Dutcher, J.P. (2002). Managing toxicities of high-dose interleukin-2. *Oncology (Williston Park)* 16 (11 Suppl 13), 11–20.
4. Howells, A., Marelli, G., Lemoine, N.R., and Wang, Y. (2017). Oncolytic viruses—interaction of virus and tumor cells in the battle to eliminate cancer. *Front. Oncol.* 7, 195.
5. Ranki, T., Pesonen, S., Hemminki, A., Partanen, K., Kairemo, K., Alanko, T., Lundin, J., Linder, N., Turkki, R., Ristimäki, A., et al. (2016). Phase I study with ONCOS-102 for the treatment of solid tumors—an evaluation of clinical response and exploratory analyses of immune markers. *J. Immunother. Cancer* 4, 17.
6. Andtbacka, R.H., Kaufman, H.L., Collichio, F., Amatruda, T., Senzer, N., Chesney, J., Delman, K.A., Spitzer, L.E., Puzanov, I., Agarwala, S.S., et al. (2015). Talimogene

- laherparepvec improves durable response rate in patients with advanced melanoma. *J. Clin. Oncol.* 33, 2780–2788.
7. Kaufman, H.L., Amatruda, T., Reid, T., Gonzalez, R., Glaspy, J., Whitman, E., Harrington, K., Nemunaitis, J., Zloza, A., Wolf, M., and Senzer, N.N. (2016). Systemic versus local responses in melanoma patients treated with talimogene laherparepvec from a multi-institutional phase II study. *J. Immunother. Cancer.* 4, 12.
 8. Formenti, S.C., and Demaria, S. (2013). Combining radiotherapy and cancer immunotherapy: a paradigm shift. *J. Natl. Cancer Inst.* 105, 256–265.
 9. Postow, M.A., Callahan, M.K., Barker, C.A., Yamada, Y., Yuan, J., Kitano, S., Mu, Z., Rasalan, T., Adamow, M., Ritter, E., et al. (2012). Immunologic correlates of the abscopal effect in a patient with melanoma. *N. Engl. J. Med.* 366, 925–931.
 10. Vacchelli, E., Bloy, N., Aranda, F., Buqué, A., Cremer, I., Demaria, S., Eggermont, A., Formenti, S.C., Fridman, W.H., Fucikova, J., et al. (2016). Trial Watch: immunotherapy plus radiation therapy for oncological indications. *OncoImmunology* 5, e1214790.
 11. Koski, A., Bramante, S., Kipar, A., Oksanen, M., Juhila, J., Vassilev, L., Joensuu, T., Kanerva, A., and Hemminki, A. (2015). Biodistribution analysis of oncolytic adenoviruses in patient autopsy samples reveals vascular transduction of noninjected tumors and tissues. *Mol. Ther.* 23, 1641–1652.
 12. Pesonen, S., Diaconu, I., Kangasniemi, L., Ranki, T., Kanerva, A., Pesonen, S.K., Gerdemann, U., Leen, A.M., Kairemo, K., Oksanen, M., et al. (2012). Oncolytic immunotherapy of advanced solid tumors with a CD40L-expressing replicating adenovirus: assessment of safety and immunologic responses in patients. *Cancer Res.* 72, 1621–1631.
 13. Santos, J.M., Havunen, R., Siurala, M., Cervera-Carrascon, V., Tähtinen, S., Sorsa, S., Anttila, M., Karell, P., Kanerva, A., and Hemminki, A. (2017). Adenoviral production of interleukin-2 at the tumor site removes the need for systemic postconditioning in adoptive cell therapy. *Int. J. Cancer* 141, 1458–1468.
 14. Hemminki, O., Parviainen, S., Juhila, J., Turkki, R., Linder, N., Lundin, J., Kankainen, M., Ristimäki, A., Koski, A., Liikanen, I., et al. (2015). Immunological data from cancer patients treated with Ad5/3-E2F-Δ24-GMCSF suggests utility for tumor immunotherapy. *Oncotarget* 6, 4467–4481.
 15. Garg, A.D., Galluzzi, L., Apetoh, L., Baert, T., Birge, R.B., Bravo-San Pedro, J.M., Breckpot, K., Brough, D., Chaurio, R., Cirone, M., et al. (2015). Molecular and translational classifications of DAMPs in immunogenic cell death. *Front. Immunol.* 6, 588.
 16. Diaconu, I., Cerullo, V., Hirvonen, M.L., Escutenaire, S., Ugolini, M., Pesonen, S.K., Bramante, S., Parviainen, S., Kanerva, A., Loskog, A.S., et al. (2012). Immune response is an important aspect of the antitumor effect produced by a CD40L-encoding oncolytic adenovirus. *Cancer Res.* 72, 2327–2338.
 17. Havunen, R., Siurala, M., Sorsa, S., Grönberg-Vähä-Koskela, S., Behr, M., Tähtinen, S., Santos, J.M., Karell, P., Rusanen, J., Nettelbeck, D.M., et al. (2016). Oncolytic adenoviruses armed with tumor necrosis factor alpha and interleukin-2 enable successful adoptive cell therapy. *Mol. Ther. Oncolytics* 4, 77–86.
 18. Siurala, M., Havunen, R., Saha, D., Lumen, D., Airaksinen, A.J., Tähtinen, S., Cervera-Carrascon, V., Bramante, S., Parviainen, S., Vähä-Koskela, M., et al. (2016). Adenoviral delivery of tumor necrosis factor-α and interleukin-2 enables successful adoptive cell therapy of immunosuppressive melanoma. *Mol. Ther.* 24, 1435–1443.
 19. Tähtinen, S., Blattner, C., Vähä-Koskela, M., Saha, D., Siurala, M., Parviainen, S., Utikal, J., Kanerva, A., Umansky, V., and Hemminki, A. (2016). T-cell therapy enabling adenoviruses coding for IL2 and TNFα induce systemic immunomodulation in mice with spontaneous melanoma. *J. Immunother.* 39, 343–354.
 20. Thomas, M.A., Spencer, J.F., La Regina, M.C., Dhar, D., Tollefson, A.E., Toth, K., and Wold, W.S. (2006). Syrian hamster as a permissive immunocompetent animal model for the study of oncolytic adenovirus vectors. *Cancer Res.* 66, 1270–1276.
 21. Balkwill, F. (2009). Tumour necrosis factor and cancer. *Nat. Rev. Cancer* 9, 361–371.
 22. Schiller, J.H., Storer, B.E., Witt, P.L., Alberti, D., Tombes, M.B., Arzooanian, R., Proctor, R.A., McCarthy, D., Brown, R.R., Voss, S.D., et al. (1991). Biological and clinical effects of intravenous tumor necrosis factor-alpha administered three times weekly. *Cancer Res.* 51, 1651–1658.
 23. Eggermont, A.M., de Wilt, J.H., and ten Hagen, T.L. (2003). Current uses of isolated limb perfusion in the clinic and a model system for new strategies. *Lancet Oncol.* 4, 429–437.
 24. Itzhaki, O., Levy, D., Zikich, D., Treves, A.J., Markel, G., Schachter, J., and Besser, M.J. (2013). Adoptive T-cell transfer in melanoma. *Immunotherapy* 5, 79–90.
 25. Dudley, M.E., Yang, J.C., Sherry, R., Hughes, M.S., Royal, R., Kammula, U., Robbins, P.F., Huang, J., Citrin, D.E., Leitman, S.F., et al. (2008). Adoptive cell therapy for patients with metastatic melanoma: evaluation of intensive myeloablative chemoradiation preparative regimens. *J. Clin. Oncol.* 26, 5233–5239.
 26. Till, B.G., Jensen, M.C., Wang, J., Chen, E.Y., Wood, B.L., Greisman, H.A., Qian, X., James, S.E., Raubitschek, A., Forman, S.J., et al. (2008). Adoptive immunotherapy for indolent non-Hodgkin lymphoma and mantle cell lymphoma using genetically modified autologous CD20-specific T cells. *Blood* 112, 2261–2271.
 27. Bramante, S., Kaufmann, J.K., Veckman, V., Liikanen, I., Nettelbeck, D.M., Hemminki, O., Vassilev, L., Cerullo, V., Oksanen, M., Heiskanen, R., et al. (2015). Treatment of melanoma with a serotype 5/3 chimeric oncolytic adenovirus coding for GM-CSF: results in vitro, in rodents and in humans. *Int. J. Cancer* 137, 1775–1783.
 28. Kanerva, A., Zinn, K.R., Chaudhuri, T.R., Lam, J.T., Suzuki, K., Uil, T.G., Hakkarainen, T., Bauerschmitz, G.J., Wang, M., Liu, B., et al. (2003). Enhanced therapeutic efficacy for ovarian cancer with a serotype 3 receptor-targeted oncolytic adenovirus. *Mol. Ther.* 8, 449–458.
 29. Moesta, A.K., Cooke, K., Piasecki, J., Mitchell, P., Rottman, J.B., Fitzgerald, K., Zhan, J., Yang, B., Le, T., Belmontes, B., et al. (2017). Local delivery of OncoVEX^{GM-CSF} generates systemic antitumor immune responses enhanced by cytotoxic T-lymphocyte-associated protein blockade. *Clin. Cancer Res.* 23, 6190–6202.
 30. Geller, M.A., and Miller, J.S. (2011). Use of allogeneic NK cells for cancer immunotherapy. *Immunotherapy* 3, 1445–1459.
 31. Seliger, B., Wollscheid, U., Momburg, F., Blankenstein, T., and Huber, C. (2001). Characterization of the major histocompatibility complex class I deficiencies in B16 melanoma cells. *Cancer Res.* 61, 1095–1099.
 32. Balasa, B., Yun, R., Belmar, N.A., Fox, M., Chao, D.T., Robbins, M.D., Starling, G.C., and Rice, A.G. (2015). Elotuzumab enhances natural killer cell activation and myeloma cell killing through interleukin-2 and TNF-α pathways. *Cancer Immunol. Immunother.* 64, 61–73.
 33. Deauvieau, F., Ollion, V., Doffin, A.C., Achard, C., Fonteneau, J.F., Verronese, E., Durand, I., Ghittoni, R., Marvel, J., Dezutter-Dambuyant, C., et al. (2015). Human natural killer cells promote cross-presentation of tumor cell-derived antigens by dendritic cells. *Int. J. Cancer* 136, 1085–1094.
 34. Lucas, M., Schachterle, W., Oberle, K., Aichele, P., and Diefenbach, A. (2007). Dendritic cells prime natural killer cells by trans-presenting interleukin 15. *Immunity* 26, 503–517.
 35. Piccioli, D., Sbrana, S., Melandri, E., and Valiante, N.M. (2002). Contact-dependent stimulation and inhibition of dendritic cells by natural killer cells. *J. Exp. Med.* 195, 335–341.
 36. Dorner, B.G., Smith, H.R., French, A.R., Kim, S., Poursine-Laurent, J., Beckman, D.L., Pingel, J.T., Kroczyk, R.A., and Yokoyama, W.M. (2004). Coordinate expression of cytokines and chemokines by NK cells during murine cytomegalovirus infection. *J. Immunol.* 172, 3119–3131.
 37. Kratochvill, F., Neale, G., Haverkamp, J.M., Van de Velde, L.A., Smith, A.M., Kawauchi, D., McEvoy, J., Roussel, M.F., Dyer, M.A., Qualls, J.E., and Murray, P.J. (2015). TNF counterbalances the emergence of M2 tumor macrophages. *Cell Rep.* 12, 1902–1914.
 38. Dannenmann, S.R., Thielicke, J., Stöckli, M., Matter, C., von Boehmer, L., Cecconi, V., Hermanns, T., Hefermehl, L., Schraml, P., Moch, H., et al. (2013). Tumor-associated macrophages subvert T-cell function and correlate with reduced survival in clear cell renal cell carcinoma. *OncoImmunology* 2, e23562.
 39. Sousa, S., Brion, R., Lintunen, M., Kronqvist, P., Sandholm, J., Monkkonen, J., Kellokumpu-Lehtinen, P.L., Lauttia, S., Tynniinen, O., Joensuu, H., et al. (2015). Human breast cancer cells educate macrophages toward the M2 activation status. *Breast Cancer Res.* 17, 101.
 40. Tähtinen, S., Grönberg-Vähä-Koskela, S., Lumen, D., Merisalo-Soikkeli, M., Siurala, M., Airaksinen, A.J., Vähä-Koskela, M., and Hemminki, A. (2015). Adenovirus improves the efficacy of adoptive T-cell therapy by recruiting immune cells to and promoting their activity at the tumor. *Cancer Immunol. Res.* 3, 915–925.

41. Patel, S.J., Sanjana, N.E., Kishton, R.J., Eidizadeh, A., Vodnala, S.K., Cam, M., Gartner, J.J., Jia, L., Steinberg, S.M., Yamamoto, T.N., et al. (2017). Identification of essential genes for cancer immunotherapy. *Nature* 548, 537–542.
42. Kanerva, A., Wang, M., Bauerschmitz, G.J., Lam, J.T., Desmond, R.A., Bhoola, S.M., Barnes, M.N., Alvarez, R.D., Siegal, G.P., Curiel, D.T., and Hemminki, A. (2002). Gene transfer to ovarian cancer versus normal tissues with fiber-modified adenoviruses. *Mol. Ther.* 5, 695–704.
43. Siurala, M., Vähä-Koskela, M., Havunen, R., Tähtinen, S., Bramante, S., Parviainen, S., Mathis, J.M., Kanerva, A., and Hemminki, A. (2016). Syngeneic syrian hamster tumors feature tumor-infiltrating lymphocytes allowing adoptive cell therapy enhanced by oncolytic adenovirus in a replication permissive setting. *Oncoimmunology* 5, e1136046.
44. Koski, A., Kangasniemi, L., Escutenaire, S., Pesonen, S., Cerullo, V., Diaconu, I., Nokisalmi, P., Raki, M., Rajecki, M., Guse, K., et al. (2010). Treatment of cancer patients with a serotype 5/3 chimeric oncolytic adenovirus expressing GMCSF. *Mol. Ther.* 18, 1874–1884.
45. Andrews, S. (2010). FastQC—a quality control tool for high throughput sequence data. Babraham Bioinformatics. <https://www.bioinformatics.babraham.ac.uk/projects/fastqc/>.
46. Ewels, P., Magnusson, M., Lundin, S., and Käller, M. (2016). MultiQC: summarize analysis results for multiple tools and samples in a single report. *Bioinformatics* 32, 3047–3048.
47. Bolger, A.M., Lohse, M., and Usadel, B. (2014). Trimmomatic: a flexible trimmer for Illumina sequence data. *Bioinformatics* 30, 2114–2120.
48. Liao, Y., Smyth, G.K., and Shi, W. (2014). featureCounts: an efficient general purpose program for assigning sequence reads to genomic features. *Bioinformatics* 30, 923–930.
49. Love, M.I., Huber, W., and Anders, S. (2014). Moderated estimation of fold change and dispersion for RNA-seq data with DESeq2. *Genome Biol.* 15, 550.
50. Zhang, B., Kirov, S., and Snoddy, J. (2005). WebGestalt: an integrated system for exploring gene sets in various biological contexts. *Nucleic Acids Res.* 33, W741–W748.
51. NCBI Resource Coordinators (2017). Database resources of the National Center for Biotechnology Information. *Nucleic Acids Res.* 45 (D1), D12–D17.
52. Brown, G.R., Hem, V., Katz, K.S., Ovetsky, M., Wallin, C., Ermolaeva, O., Tolstoy, I., Tatusova, T., Pruitt, K.D., Maglott, D.R., and Murphy, T.D. (2015). Gene: a gene-centered information resource at NCBI. *Nucleic Acids Res.* 43, D36–D42.
53. Zivcec, M., Safronetz, D., Haddock, E., Feldmann, H., and Ebihara, H. (2011). Validation of assays to monitor immune responses in the Syrian golden hamster (*Mesocricetus auratus*). *J. Immunol. Methods* 368, 24–35.
54. Tähtinen, S., Kaikkonen, S., Merisalo-Soikkeli, M., Grönberg-Vähä-Koskela, S., Kanerva, A., Parviainen, S., Vähä-Koskela, M., and Hemminki, A. (2015). Favorable alteration of tumor microenvironment by immunomodulatory cytokines for efficient T-cell therapy in solid tumors. *PLoS ONE* 10, e0131242.

OMTO, Volume 11

Supplemental Information

Abscopal Effect in Non-injected Tumors

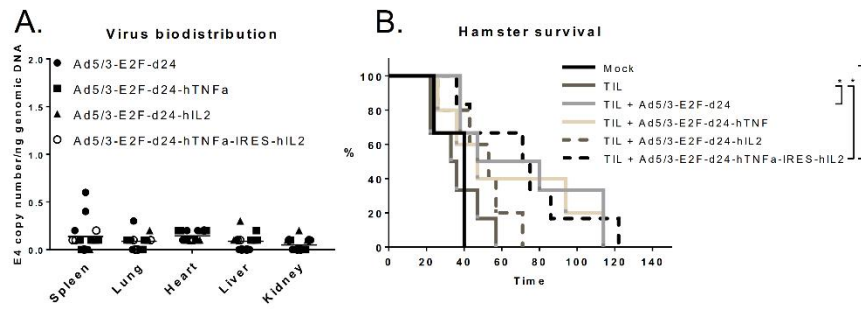
Achieved with Cytokine-Armed Oncolytic

Adenovirus

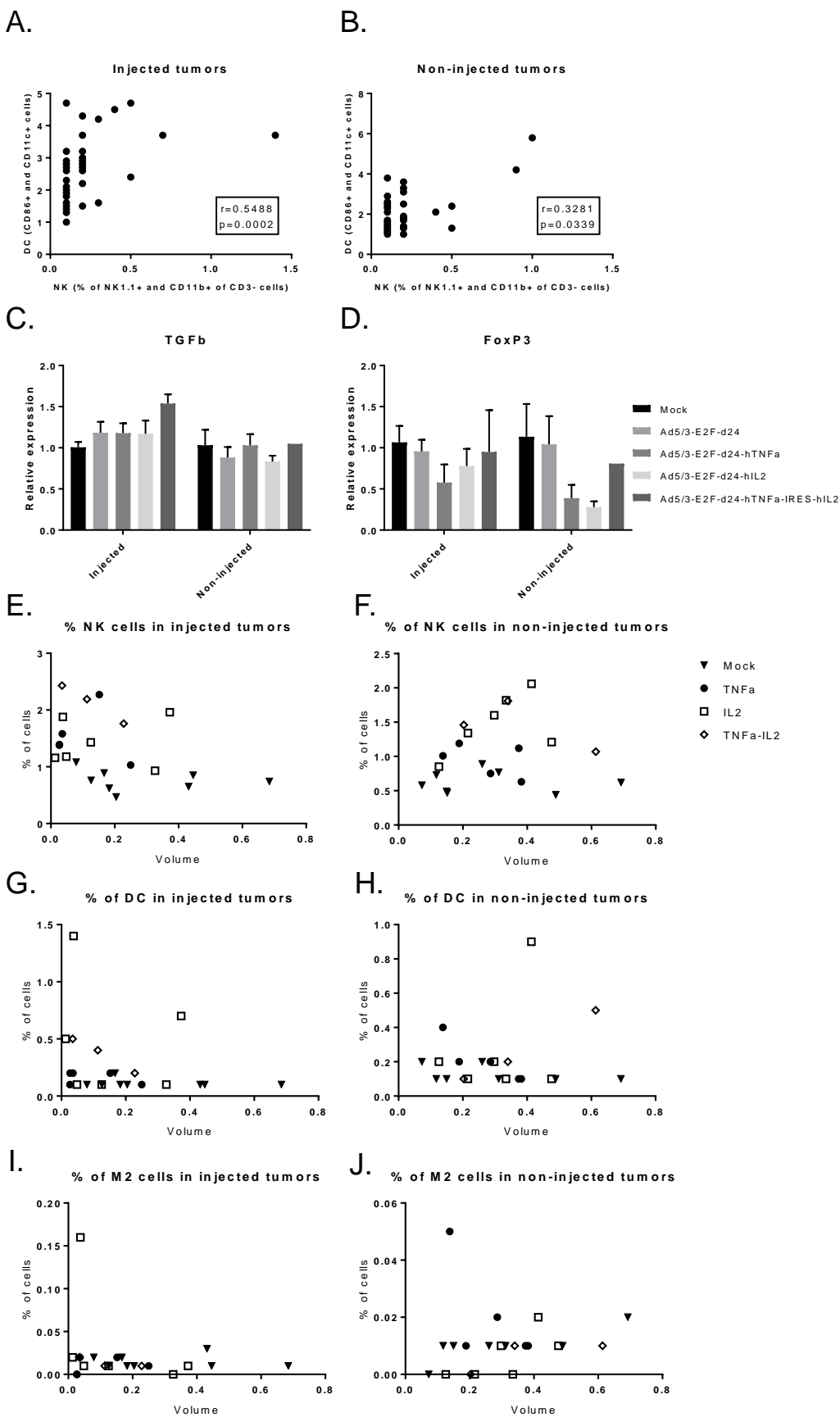
Riikka Havunen, João M. Santos, Suvi Sorsa, Tommi Rantaperö, Dave Lumen, Mikko Siurala, Anu J. Airaksinen, Victor Cervera-Carrascon, Siri Tähtinen, Anna Kanerva, and Akseli Hemminki

Supplementary Materials:

Fig. S1

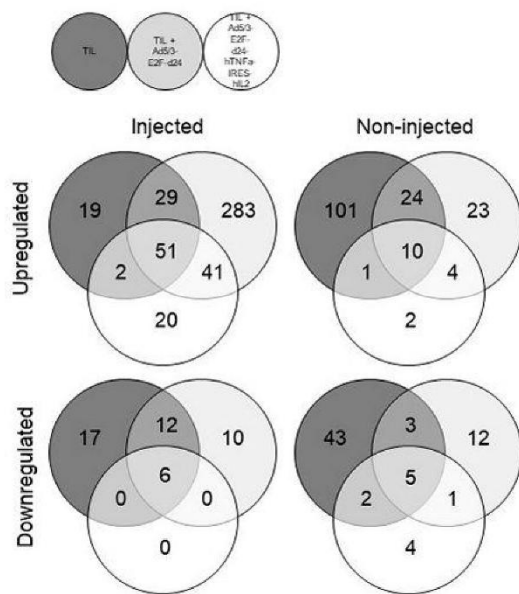


Supplementary Figure S1. Viruses spread throughout the body and prolong hamster survival. Small amounts of viral DNA were detected in different parts of the body on day 16 (A). The tumor progression of the hamsters treated with viruses on days 1, 8, 15, 22, and 29, and once with TILs was followed until the tumor size exceeded 2.0 cm or the tumors ulcerated (B). Log-rank test was performed to evaluate the statistical significance, * $p < 0.05$.



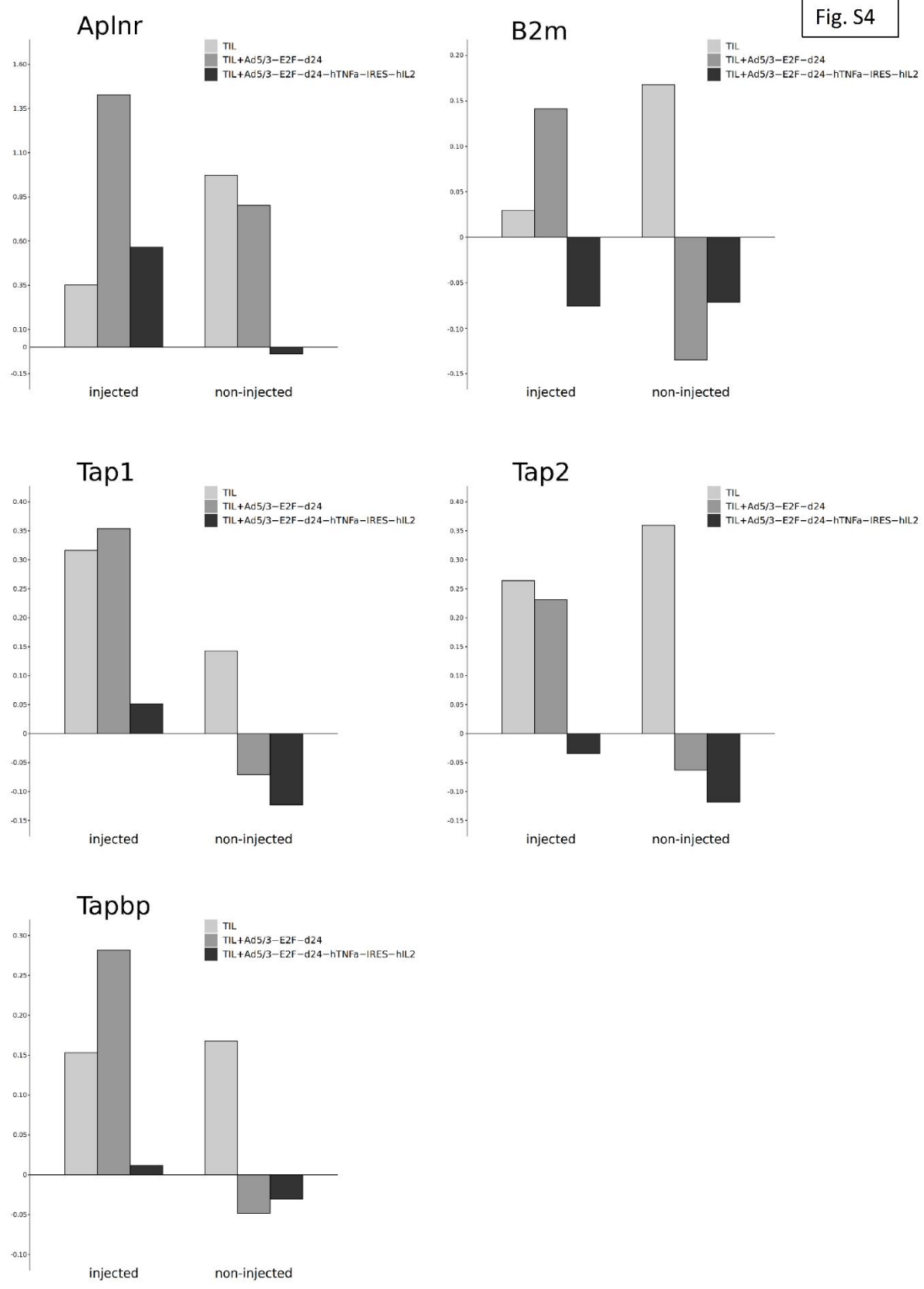
Supplementary Figure S2. The level of dendritic cells in the tumor positively correlates with the level of NK cells. The correlation was determined with Spearman's rank correlation equation (A, B). Relative gene expression levels of TGFb (C) and FoxP3 (D) in injected or non-injected tumors. Mean plus SEM is shown. Percentage of immune cells in tumors (NK cells (E, F), DCs (G, H) and M2 macrophages (I, J) in injected and non-injected tumors, respectively) did not correlate with tumor volumes.

Fig. S3



Supplementary figure S3. Number of differentially expressed genes in tumors compared with corresponding mock tumors. The number inside a restricted area describes the number of differentially expressed genes unique in a group or common between two or three groups.

Fig. S4



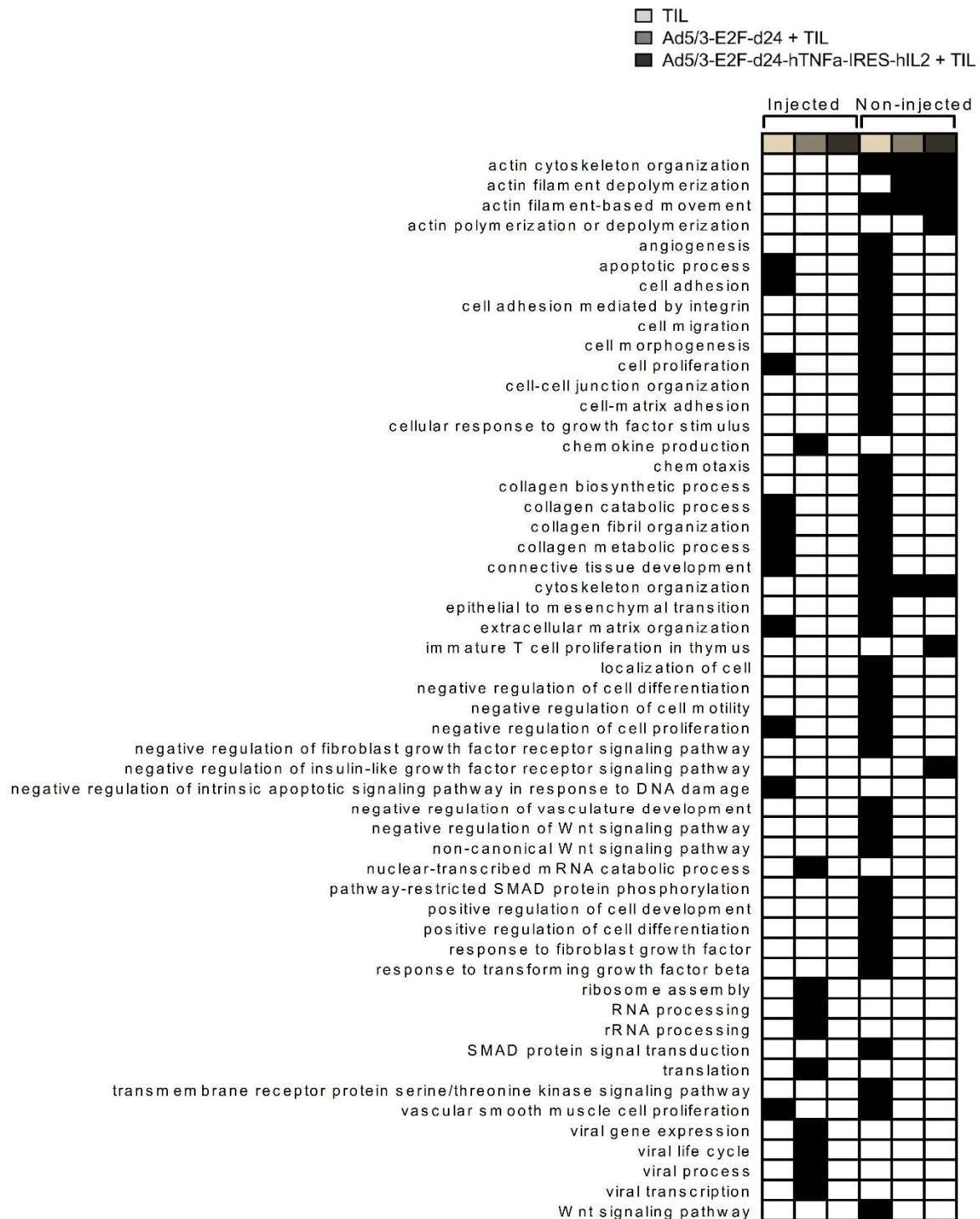
Supplementary figure S4. Change in the expression of essential genes for immunotherapy. Log2 fold-change of selected immunotherapy-related genes compared with the corresponding mock group.

Fig. S5

- TIL
- Ad5/3-E2F-d24 + TIL
- Ad5/3-E2F-d24-hTNFa-IRES-hIL2 + TIL



Fig. S6



Supplementary figure S6. Downregulated genes are related to various processes in cells. Gene ontology analysis was performed to group the downregulated genes according to their functions. Black box indicates the treatment groups where the downregulation of the pathway was observed.

Supplementary Table S1. Saline injection induces changes in immunologically relevant gene sets. Gene ontology classification was performed against human genome for human orthologs. Most relevant gene groups are shown for both up- and downregulated genes.

UPREGULATED			
Geneset	Description	FDR	Genes
GO:0009617	response to bacterium	0.001884	ADM; CSF3; HPGD; LCN2; S100A8; S100A9; CXCL5; SFTPD; TNF; PGLYRP1
GO:0006955	immune response	0.00336	ADM; CSF3; CFD; LCN2; ENPP3; PIGR; PLSCR1; IL20RB; S100A8; S100A9; CXCL5; SFTPD; TNF; C3; PGLYRP1
GO:0051707	response to other organism	0.00355	ADM; CSF3; HPGD; LCN2; PLSCR1; S100A8; S100A9; CXCL5; SFTPD; TNF; PGLYRP1
GO:0043207	response to external biotic stimulus	0.00355	ADM; CSF3; HPGD; LCN2; PLSCR1; S100A8; S100A9; CXCL5; SFTPD; TNF; PGLYRP1
GO:0009607	response to biotic stimulus	0.004028	ADM; CSF3; HPGD; LCN2; PLSCR1; S100A8; S100A9; CXCL5; SFTPD; TNF; PGLYRP1
GO:0042592	homeostatic process	0.004028	ADM; CP; FGF12; GCK; HCAR2; LCN2; SLC26A4; PIGR; IL20RB; S100A8; S100A9; SFTPD; SLC9A3; TNF; NAPSA
GO:0052547	regulation of peptidase activity	0.004281	WFDC2; PI16; FETUB; S100A8; S100A9; SFRP2; TNF; C3
GO:0002682	regulation of immune system process	0.00633	CSF3; CFD; DPP4; HCAR2; PIGR; PLSCR1; IL20RB; CXCL5; SFTPD; BMP5; TNF; C3; PGLYRP1
GO:0051050	positive regulation of transport	0.006421	CSF3; FGF12; GCK; EHD3; HCAR2; S100A8; S100A9; SFRP2; SFTPD; TNF; C3
GO:0032496	response to lipopolysaccharide	0.006421	ADM; CSF3; HPGD; LCN2; S100A8; CXCL5; TNF
GO:0002237	response to molecule of bacterial origin	0.007698	ADM; CSF3; HPGD; LCN2; S100A8; CXCL5; TNF
GO:0042742	defense response to bacterium	0.009877	ADM; S100A8; S100A9; SFTPD; TNF; PGLYRP1
GO:0002526	acute inflammatory response	0.010866	PLSCR1; IL20RB; S100A8; TNF; C3
GO:0002861	regulation of inflammatory response to antigenic stimulus	0.010866	IL20RB; TNF; C3
GO:0006952	defense response	0.012188	ADM; CFD; DPP4; LCN2; PLSCR1; IL20RB; S100A8; S100A9; CXCL5; SFTPD; TNF; C3; PGLYRP1
GO:0052548	regulation of endopeptidase activity	0.013068	WFDC2; FETUB; S100A8; S100A9; SFRP2; TNF; C3
GO:0048878	chemical homeostasis	0.01554	ADM; CP; FGF12; GCK; LCN2; SLC26A4; S100A8; S100A9; SFTPD; SLC9A3; NAPSA
GO:0046916	cellular transition metal ion homeostasis	0.024977	CP; LCN2; S100A8; S100A9
GO:0050832	defense response to fungus	0.029304	ADM; S100A8; S100A9
GO:0050727	regulation of inflammatory response	0.035014	IL20RB; S100A8; S100A9; TNF; C3; PGLYRP1
GO:0098542	defense response to other organism	0.035375	ADM; PLSCR1; S100A8; S100A9; SFTPD; TNF; PGLYRP1
GO:0002437	inflammatory response to antigenic stimulus	0.048265	IL20RB; TNF; C3

GO:0006954	inflammatory response	0.048265	PLSCR1; IL20RB; S100A8; S100A9; CXCL5; TNF; C3; PGLYRP1
GO:0050729	positive regulation of inflammatory response	0.048265	S100A8; S100A9; TNF; C3
GO:0055076	transition metal ion homeostasis	0.048265	CP; LCN2; S100A8; S100A9
GO:0009605	response to external stimulus	0.048265	ADM; CSF3; HPGD; LCN2; PLSCR1; IL20RB; S100A8; S100A9; CXCL5; SFRP2; SFTPD; TNF; C3; PGLYRP1
GO:0002883	regulation of hypersensitivity	0.048265	IL20RB; C3
GO:0043129	surfactant homeostasis	0.048265	SFTPD; NAPSA
GO:0050766	positive regulation of phagocytosis	0.048553 0	SFTPD; TNF; C3

DOWNREGULATED

Geneset	Description	FDR	Genes
GO:0030048	actin filament-based movement	0	DES; MYBPC1; MYH3; MYH8; MYL1; MYL2; MYL3; NEB; ATP1A2; ACTA1; SCN5A; ACTC1; TMOD1; TNNC2; TNNC1; TNNI1; TNNT1; TNNT2; TNNT3; TPM2; TTN; CACNA2D1; TCAP; CAV3; ACTN2
GO:0007010	cytoskeleton organization	1.02E-11	KLHL41; CAP2; NES; CORO1A; LDB3; ADD2; XIRP2; CRYAB; XIRP1; DES; SYNPO2; FGD2; ANKRD1; PDLIM3; ANK1; KIT; MEF2C; LMOD2; MYH3; MYL2; NEB; MYOZ2; PFN2; PKP1; WNT4; LMOD3; PROX1; TRIM54; ACTA1; CCL11; CCL21; SPTB; ACTC1; TMOD1; TNNT2; TPM2; TTN; SYNPO2L; CSRP3; OBSCN; CASQ1; CASQ2; MYPN; GPR65; TCAP; CAV3; ACTN2; NEXN
GO:0007015	actin filament organization	6.42E-10	CAP2; CORO1A; ADD2; SYNPO2; PDLIM3; LMOD2; PFN2; WNT4; LMOD3; PROX1; ACTA1; CCL11; CCL21; SPTB; ACTC1; TMOD1; TNNT2; TPM2; TTN; SYNPO2L; GPR65; TCAP; CAV3; ACTN2
GO:0008015	blood circulation	3.00E-09	DES; EPHX2; F5; HSPB7; HRC; CXCL10; AR; KCNJ11; MYL1; MYL2; MYL3; ATP1A2; RYR1; SCN5A; SLC8A1; ACTC1; TNNC1; TNNI1; TNNT2; TTN; CACNA1S; CACNA2D1; CACNG1; CSRP3; CASQ1; CASQ2; TCAP; CAV3
GO:0051495	positive regulation of cytoskeleton organization	3.78E-05	NES; CORO1A; SYNPO2; LMOD2; PFN2; WNT4; PROX1; CCL11; CCL21; SYNPO2L; GPR65; CAV3; ACTN2
GO:0030335	positive regulation of cell migration	5.54E-04	CORO1A; FLT4; DAPK2; HSPB1; CXCL10; ITGA4; KIT; PGF; PROX1; RELN; ACKR3; CCL11; CCL21; SLC8A1; THBS4; WNT7A; CXCL14
GO:0051494	negative regulation of cytoskeleton organization	8.31E-04	CORO1A; ADD2; LMOD2; PFN2; LMOD3; TRIM54; SPTB; TMOD1; CAV3
GO:0008154	actin polymerization or depolymerization	0.001091 6	CAP2; CORO1A; ADD2; LMOD2; PFN2; LMOD3; CCL11; CCL21; SPTB; TMOD1; ACTN2
GO:0090136	epithelial cell-cell adhesion	0.001426 3	CYP1B1; KIT; NOV; THBS4
GO:0006887	exocytosis	0.001890 9	CPLX2; CORO1A; CTSW; F5; MMRN1; ANK1; KIT; TRIM72; PFN2; SERPINA1; RAB27A; TIMP3; TTN; ZAP70; ACTN2; SYTL3

GO:0030837	negative regulation of actin filament polymerization	0.002007 3	ADD2; LMOD2; PFN2; LMOD3; SPTB; TMOD1
GO:0030217	T cell differentiation	0.002663 5	IHH; KIT; LCK; WNT4; SATB1; SPN; ZAP70; EOMES; FZD8; CD3E; CD8A
GO:0045321	leukocyte activation	0.003304 7	IKZF1; CPLX2; CORO1A; SH2D1B; IHH; ITGA4; KIT; LCK; MEF2C; WNT4; RAB27A; SATB1; CCL21; SPN; ZAP70; TNFAIP8L2; EOMES; FZD8; CD3E; CD8A; ITM2A; CD40
GO:0051693	actin filament capping	0.003319 5	ADD2; LMOD2; LMOD3; SPTB; TMOD1
GO:0002521	leukocyte differentiation	0.006935 9	IKZF1; IHH; ITGA4; KIT; LCK; MEF2C; WNT4; FAM20C; SATB1; SPN; ZAP70; EOMES; FZD8; CD3E; CD8A; ITM2A
GO:0002551	mast cell chemotaxis	0.007554 4	KIT; PGF; CCL11
GO:0050900	leukocyte migration	0.007652 7	CORO1A; DAPK2; CXCL10; ITGA4; KIT; LCK; NOV; PGF; CCL11; CCL21; SPN; THBS4; ZAP70; CXCL14
GO:0008284	positive regulation of cell proliferation	0.008454 5	NES; CORO1A; FLT4; IHH; CXCL10; AR; KIT; MEF2C; PGF; PROX1; CLEC11A; SCN5A; CCL11; ST8SIA1; SPN; TGM2; THBS4; WNT7A; ZAP70; CAV3; ALDH1A2; CD3E; CD40
GO:0007159	leukocyte cell-cell adhesion	0.009966 9	CORO1A; IHH; ITGA4; KIT; LCK; WNT4; RAB27A; SATB1; CCL21; SPN; ZAP70; TNFAIP8L2; EOMES; FZD8; CD3E; CD8A
GO:0001568	blood vessel development	0.010149 6	CSPG4; CYP1B1; FLT4; HSPB1; CXCL10; MEF2C; NOV; PGF; WNT4; PROX1; ACKR3; CCL11; THBS4; C6; WNT7A; WT1; FZD8; ALDH1A2
GO:0042110	T cell activation	0.012012 6	CORO1A; IHH; KIT; LCK; WNT4; RAB27A; SATB1; CCL21; SPN; ZAP70; TNFAIP8L2; EOMES; FZD8; CD3E; CD8A
GO:0043383	negative T cell selection chemotaxis	0.012118 8	SPN; ZAP70; CD3E
GO:0006935	positive regulation of chemotaxis	0.013243 7	CORO1A; DAPK2; HSPB1; CXCL10; KIT; MATN2; NOV; PGF; RELN; ACKR3; CCL11; CCL21; SPN; SPTB; THBS4; BOC; CXCL14
GO:0050921	positive regulation of intracellular signal transduction	0.020007 2	DAPK2; HSPB1; CXCL10; PGF; CCL21; THBS4; CXCL14
GO:1902533	myeloid leukocyte migration	0.020882 5	ABRA; CSPG4; CYP1B1; FGD2; FLT4; ANKRD1; LMCD1; CXCL10; AR; KIT; LCK; RELN; ACKR3; CCL11; CCL21; TGM2; WNT7A; ZAP70; FZD8; GPR65; CD3E; CD8A; CD40
GO:0097529	insulin-like growth factor receptor signaling pathway	0.022119 0	DAPK2; CXCL10; KIT; NOV; PGF; CCL11; CCL21; THBS4
GO:0048009	MAPK cascade	0.027582 4	GRB10; AR; TRIM72; CILP
GO:0000165	T cell migration	0.027703 2	CRYAB; CSPG4; FGD2; FLT4; GFRA2; AR; KIT; MEF2C; ACKR3; NDRG2; CCL11; CCL21; SPTB; TIMP3; WNT7A; DUSP26; CAMK2A; CAMK2B; FZD8; CAV3; ACTN2; CD40
GO:0072678	T cell migration	0.031876 2	CXCL10; ITGA4; CCL21; ZAP70

GO:0043299	leukocyte degranulation	0.034746 2	CPLX2; CORO1A; KIT; RAB27A; ZAP70
GO:0012501	programmed cell death	0.036414 8	NES; CORO1A; CRYAB; CYP1B1; EEF1A2; FGD2; FLT4; DAPK2; ANKRD2; ANKRD1; BIN1; HSPB1; IHH; IRF5; AR; KIT; LCK; MEF2C; PEG3; WNT4; ACKR3; SATB1; CCL21; SPN; ACTC1; TGM2; TIMP3; UCP2; WNT7A; WT1; CAMK2A; OBSCN; GPR65; ACTN2; ALDH1A2; CD3E; CD40
GO:0002520	immune system development	0.041954 7	IKZF1; ADD2; GPR171; IHH; ITGA4; KIT; LCK; MB; MEF2C; WNT4; FAM20C; SATB1; SPN; ZAP70; EOMES; FZD8; CD3E; CD8A; ITM2A; CD40
GO:0001525	angiogenesis	0.043340 3	CSPG4; CYP1B1; FLT4; HSPB1; CXCL10; NOV; PGF; ACKR3; CCL11; THBS4; C6; WNT7A; FZD8
GO:0070661	leukocyte proliferation	0.044425 0	CORO1A; IHH; KIT; MEF2C; WNT4; SATB1; SPN; ZAP70; CD3E; CD40
GO:0006955	immune response	0.045732 8	IL18BP; PRG4; CPLX2; CORO1A; SH2D1B; CTSW; FCGR3A; MYLPPF; CXCL10; IRF5; ITGA4; KIT; LCK; MEF2C; RAB27A; CCL11; CCL21; SPN; C6; C7; ZAP70; TNFAIP8L2; CAMK2A; CAMK2B; EOMES; GPR65; CD3E; CD8A; ITM2A; CXCL14; CD40

Supplementary Table S2. Injection with Ad5/3-E2F-d24-hTNFa-IRES-hIL2 induces a gene-expression profile unique for both injected and non-injected tumors. Significantly ($p < 0.05$) upregulated or downregulated genes found both in injected and non-injected tumors only in the group treated with Ad5/3-E2F-d24-hTNFa-IRES-hIL2.

Gene	Name	Function
UPREGULATED		
<i>Avil</i>	Advillin	Actin regulatory protein
<i>Cebpg</i>	CCAAT/enhancer-binding protein gamma	Suppresses senescence and inflammatory gene expression by heterodimerizing with C/EBP β
<i>Csf3</i>	Colony Stimulating Factor 3	Production, differentiation, and function of granulocytes
<i>Cxcl5</i> (LOC101835923)	Alveolar macrophage chemotactic factor	Chemokine induced by TNFa
<i>Gnb3</i>	Guanine nucleotide-binding protein G(I)/G(S)/G(T) subunit beta-3	G protein, cell signaling
<i>Hapln1</i>	Hyaluronan and proteoglycan link protein 1	Stabilizes proteoglycan monomers
<i>Ier3</i>	Radiation-inducible immediate-early gene IEX-1	Induced by cytokines and viral infection Induces TNFa-stimulated apoptosis Inhibits T cell apoptosis
LOC101834995	Ribosomal protein S6 kinase beta-1 pseudogene	
<i>Lrmp</i>	Lymphoid-restricted membrane protein	Delivers peptides to major histocompatibility complex class I molecules
<i>Pdk1</i>	Pyruvate dehydrogenase lipoamide kinase isozyme 1, mitochondrial	General metabolism
<i>Ptprm</i>	Receptor-type tyrosine-protein phosphatase mu	Regulates cell growth, differentiation, mitotic cycle, and oncogenic transformation
<i>Rev1</i>	DNA repair protein REV1	Involved in DNA damage reparation
<i>Rgs13</i>	Regulator of G-protein signaling 13	Regulates expansion and differentiation of naive B cells
<i>Rnase2</i>	Eosinophil-derived neurotoxin	Non-secretory ribonuclease, chemotactic for dendritic cells
<i>Sult1e1</i>	Estrogen sulfotransferase	Regulates inflammatory response
<i>Trpm5</i>	Transient receptor potential cation channel subfamily M member 5	Ion channel
DOWNREGULATED		
<i>Bscl2</i>	Seipin	Involved in adipogenesis, lipid droplet homeostasis and cellular triglyceride lipolysis
<i>Camsap3</i>	Calmodulin-regulated spectrin-associated protein 3	Microtubule minus-end binding protein
<i>Card14</i>	Caspase recruitment domain-containing protein 14	Forms molecular scaffolds for the assembly of multiprotein complexes

Desi1	Desumoylating Isopeptidase 1	Deconjugates substrates from SUMO proteins
Jak3	Janus kinase 3	Expressed in T cells and NK cells, mediates IL2R signaling
Khsrp	Far upstream element-binding protein 2	RNA-binding protein that stabilizes for example cytokine mRNAs
Lap3	Leucine Aminopeptidase 3	Functions in intracellular protein processing.
LOC101824821	Guanylate-binding protein 2-like	
LOC101825087	Guanylate-binding protein 4-like	
LOC101826062	H-2 class I histocompatibility antigen, alpha chain-like	
LOC101828355	H-2 class II histocompatibility antigen, E-U alpha chain	Antigen presentation
LOC101834191	Interferon-inducible GTPase 1-like	
LOC101834868	Rano class II histocompatibility antigen, A beta chain-like	
LOC101835956	Chromosome unknown C19orf66 homolog	
LOC101837226	Immunity-related GTPase family M protein 1-like	
LOC101838705	Chromosome unknown C16orf92 homolog	
LOC101844521	Class II histocompatibility antigen, M beta 1 chain	Antigen presentation
LOC101844787	Class II histocompatibility antigen, M alpha chain	Antigen presentation
LOC106022816	Uncharacterized	
Rpl7l1	Ribosomal protein L7 like 1	mRNA translation
Smg5	SMG5, Nonsense Mediated MRNA Decay Factor	Functions in mRNA degradation
Uhrf1	Ubiquitin-like, containing PHD and RING finger domains, 1	Functions in p53-dependent DNA damage checkpoint
Wars	Tryptophanyl-tRNA synthetase, cytoplasmic	Catalyzes the aminoacylation of tRNA with tryptophan and is induced by interferons